

**Fe<sub>3</sub>O<sub>4</sub>/ZrO<sub>2</sub> NANOCOMPOSITE MODIFIED CARBON PASTE  
ELECTRODE; PREPARATION, CHARACTERIZATION AND  
APPLICATION FOR THE DETECTION OF ASCORBIC ACID**

**MSc THESIS**

**GENET BEKELE SIME**

**JUNE 2018**

**HARAMAYA UNIVERSITY, HARAMAYA**

**Fe<sub>3</sub>O<sub>4</sub>/ZrO<sub>2</sub> Nanocomposite Modified Carbon Paste Electrode; Preparation,  
Characterization and Application for the Detection of Ascorbic Acid**

**A Thesis Submitted to the Department of Chemistry, Postgraduate Program**

**Directorate**

**HARAMAYA UNIVERSITY**

**In partial Fulfillment of the Requirements for the Degree of**

**MASTER OF SCIENCE IN CHEMISTRY**

**(PHYSICAL CHEMISTRY)**

**Genet Bekele Sime**

**June 2018**

**Haramaya University, Haramaya**



## **DEDICATION**

I dedicate this Thesis work to my Family, who had given unlimited aid and treated me with love and affection.

## STATEMENT OF THE AUTHOR

By my signature below, I declare and affirm that this Thesis is my own work. I have followed all ethical and technical principles of scholarship in the preparation, data collection, data analysis and compilation of this Thesis. Any scholarly matter that is included in the Thesis has been given recognition through citation.

This Thesis is submitted in partial fulfillment of the requirements for an MSc degree at the Haramaya University. The thesis is deposited in the Haramaya University Library and is made available to borrowers under the rules of the Library. I solemnly declare that this Thesis has not been submitted to any other institution anywhere for the award of any academic degree, diploma or certificate.

Brief quotations from this Thesis may be made without special permission provided that accurate and complete acknowledgment of the source is made. Requests for permission for extended quotation from or reproduction of this Thesis in whole or part may be granted by the Head of the Department or Director of the Postgraduate Program Directorate when in his or her judgment the proposed use of material is in the interest of scholarship. In all other instances, however, permission must be obtained from the author of the Thesis.

Name: Genet Bekele

Signature: \_\_\_\_\_

Date: \_\_\_\_\_

Department: Chemistry

## **BIOGRAPHICAL SKETCH OF THE AUTHOR**

The author of this thesis, Genet Bekele, was born on June 28, 1993 in Robe Town Bale Zone of Oromia Regional State, from her father Ato Bekele Sime and mother W/ro Tsige Reta. She attended her primary school in Amanuel Elementary School, Robe, and her secondary school in Robe Secondary and Preparatory School. After successfully passing Ethiopian School Leaving Certificate Examination (ESLCE) she joined Jimma University in 2012/13 and graduated with BSc degree in Chemistry in 2015. The following year she was assigned by Ministry of Education as Graduate Assistant and subsequently in the same year she joined the Postgraduate Program Directorate of Haramaya University to pursue her MSc study in chemistry (physical).

## ACKNOWLEDGEMENTS

Above all, I would like to thank the Almighty God and his beloved mother Holy Saint Virgin Mary for their kind-hearted help in all aspects of my life in combination with blessing and supplying strength and always lifting me up.

First and for most, I would like to express my deep and sincere gratitude to my major advisors, Dr. Abebaw Adgo for his continuous encouragement, advice, valuable discussion and arranging facilities without hesitation and their warm assistance and support throughout my research study. Besides, I also thank his critical comments on the courses, seminars and thesis work. I am also very much grateful to my co-advisor Dr. Endale Teju for his valuable comments excellent advice, and very kind approach. They shared their own huge life experiences and gave me energy and stimuli to finish my research.

I also would like to extend my acknowledgement to Dr. Abi Tadesse for providing characterizing the nanomaterials by SEM-EDX and share so many hours of encouraging and invaluable advice with out in reservation and insight throughout my studies. Besides, I also appreciate his critical comments and constructive criticism given to me.

I would like to express my thanks to Haramaya University, Department of Chemistry for providing instruments with full Laboratory facility and facilitating with different things from initial to end of this postgraduate program study and similar thanks to Ministry of Education sponsoring me for the study. I would like to thank Addis Ababa University, Department of Chemistry, for their cooperation in running the FTIR and XRD analysis.

Finally, I would like to thank all the member of my lovely family for their endless love and moral support throughout my life and during the study period.

## ACRONYMS AND ABBREVIATIONS

AA	Ascorbic Acid
ABS	Acetate Buffer Solution
CPE	Carbon Paste Electrode
CV	Cyclic Voltammetry
DPV	Differential Pulse Voltammetry
EIS	Electrochemical Impedance Spectroscopy
Epa	Anodic peak potential
GCE	Glassy Carbon electrode
Ipa	Anodic peak current
LOD	Limit of Detection
MCPE	Modified Carbon Paste Electrode
RSD	Relative Standard Deviation
SEM	Scanning Electron Microscopy
XRD	X-ray Diffractometry

## TABLE OF CONTENTS

<b>STATEMENT OF THE AUTHOR</b>	<b>iv</b>
<b>BIOGRAPHICAL SKETCH OF THE AUTHOR</b>	<b>v</b>
<b>ACKNOWLEDGEMENTS</b>	<b>vi</b>
<b>ACRONYMS AND ABBREVIATIONS</b>	<b>vii</b>
<b>TABLE OF CONTENTS</b>	<b>viii</b>
<b>LIST OF TABLES</b>	<b>xi</b>
<b>LIST OF FIGURES</b>	<b>xii</b>
<b>LIST OF TABLES IN THE APPENDIX</b>	<b>xiv</b>
<b>ABSTRACT</b>	<b>xv</b>
<b>1. INTRODUCTION</b>	<b>1</b>
<b>2. LITERATURE REVIEW</b>	<b>5</b>
2.1. Ascorbic Acid	5
2.2. Detection Methods of Ascorbic Acid	6
2.2.1. Ascorbic Acid Detection by Spectroscopic Techniques	6
2.2.2. Ascorbic Acid Detection by Electrochemical Techniques	7
2.3. Sensors	9
2.3.1. Electrochemical Sensors	10
2.3.2. Amperometric Sensors	10
2.3.3. Conductometric Sensors	10
2.4. Carbon Paste Electrodes	11
2.5. Chemically Modified Carbon Paste Electrode	12
2.6. Nanoparticle	13
2.7. Metal Oxide Nanoparticles	14
2.7.1. Carbon Material Based Electrochemical Sensors	15
2.8. Synthesis Techniques of Nanocomposite	15
2.8.1. Co-Precipitation Method	15
2.8.2. Sol-Gel Method	16

2.8.3. Hydrothermal Method	16
2.9. Electrochemical Characterization	16
2.9.1. Cyclic Voltammetry (CV)	16
2.9.2. Electrochemical Impedance Spectroscopy (EIS)	18
2.9.3. Differential Pulse Voltammetry (DPV)	20
<b>3. MATERIALS AND METHODS</b>	<b>22</b>
3.1. Experimental Sites	22
3.2. Instruments and Apparatus	22
3.3. Chemicals and Reagent	22
3.4. Procedures for the Synthesis of Nanomaterials	23
3.4.1. Synthesis of Fe <sub>3</sub> O <sub>4</sub> Nanoparticles	23
3.4.2. Synthesis of ZrO <sub>2</sub> Nanoparticles	23
3.4.3. Synthesis of Fe <sub>3</sub> O <sub>4</sub> /ZrO <sub>2</sub> Nanocomposite	24
3.4.4. Preparation of Carbon Paste Electrode	24
3.4.5. Preparation of Fe <sub>3</sub> O <sub>4</sub> , ZrO <sub>2</sub> and Fe <sub>3</sub> O <sub>4</sub> /ZrO <sub>2</sub> nanocomposite Modified Carbon Paste Electrode	24
3.5. Preparation of Acetate Buffer Solutions	25
3.6. Electrochemical Characterization of Nanocomposites	25
3.7. Spectroscopic Characterization	25
3.8.1. Influence of pH	26
3.8.2. Influence of Concentration	26
3.9. Determination of Ascorbic Acid	26
3.10. Method Detection Limit	26
<b>4. RESULTS AND DISCUSSION</b>	<b>27</b>
4.1. Structural and Morphological Characterization of as Produced Nanomaterials	27
4.1.1. XRD Analysis	27
4.1.2. Scanning Electron Microscopy (SEM)	28
4.1.3. FTIR Analysis	29
4.1.1. UV-Vis Results Analysis	30
4.2. Electrochemical Investigation	31
4.2.1. Potential Windows of Electrode Features	31

4.2.2. Cyclic Voltammetry of Potassium Ferricyanide on Varies Modified CPE	33
4.2.3. Electrochemical Impedance Spectroscopy	37
4.3. Electrochemical Behavior of Ascorbic Acid at the Surface of Various Electrodes	38
4.4. The Electrochemical Response of AA at $\text{Fe}_3\text{O}_4/\text{ZrO}_2/\text{CPE}$	39
4.5. Optimization of Experimental Parameters for Ascorbic Acid Detection	40
4.5.1. Effect of Scan Rate	40
4.5.2. Effect of pH	42
4.6. Application of $\text{Fe}_3\text{O}_4/\text{ZrO}_2/\text{CPE}$ Electrode for the Determination of AA	43
4.7. Detection of Ascorbic Acid in paracetamol	45
4.8. Reproducibility and Stability	45
<b>5. SUMMARY, CONCLUSION AND RECOMMENDATION</b>	<b>47</b>
5.1. Summary and Conclusion	47
5.2. Recommendation	48
<b>6. REFERENCES</b>	<b>49</b>
<b>7. APPENDIXES</b>	<b>64</b>

## LIST OF TABLES

<b>Table</b>	<b>Page</b>
1. Advantages and Limitation of Carbon Paste Electrode	12
2. The effect of scan rate on peak current using CPE in 2 mM $K_3Fe(CN)_6$	35
3. The effect of scan rate on peak current using $Fe_3O_4/CPE$ in 2 mM $K_3Fe(CN)_6$	36
4. The effect of scan rate on peak current using $ZrO_2/CPE$ in 2 mM $K_3Fe(CN)_6$	36
5. The effect of scan rate on peak current using $Fe_3O_4/ZrO_2/CPE$ in 2 mM $K_3Fe(CN)_6$	36
6. Comparison of the present work with previous reported ones	44

## LIST OF FIGURES

<b>Figure</b>	<b>Page</b>
1. The chemical structure of ascorbic acid	5
2. Oxidation of ascorbic acid	8
3. Cyclic voltammograms obtained with a Pt working electrode for different ascorbic acid concentrations	9
4. A typical cyclic voltammogram depicting oxidation and reduction peaks of an analyte between specified values of $E_i$ and $E_f$ (in tis case -0.5 to 0.5 V).	17
5. Cyclic voltammetry profiles for (A) reversible, (B) irreversible and (C) quasireversible processes.	18
6. Electrochemical impedance depicted by (A) the Nyquist plot and (B) Bode plot	20
7. Potential wave form and response for DPV	21
8. XRD pattern of (a) $ZrO_2$ , (b) $Fe_3O_4$ nanoparticles and (c) $Fe_3O_4/ZrO_2$ nanocomposite	28
9. SEM-EDX images of $ZrO_2$ and $Fe_3O_4/ZrO_2$ nanocomposite	29
10. FTIR spectra of a) $ZrO_2$ b) $Fe_3O_4$ nanoparticles and c) $Fe_3O_4/ZrO_2$ nanocomposite	30
11. UV-Vis spectra of $Fe_3O_4$ , $ZrO_2$ nanoparticles and $Fe_3O_4/ZrO_2$ nanocomposite	31
12. Potential Windows CVs of various electrodes in aq. KCl (0.1 M), $\nu = 100 \text{ mVs}^{-1}$	33
13. CVs of a) CPE, b) $Fe_3O_4/CPE$ , c) $ZrO_2/CPE$ and d) $Fe_3O_4/ZrO_2/CPE$ (at 10, 25, 50, 75 and $100 \text{ mV s}^{-1}$ scan rates) in 2 mM of $K_3Fe(CN)_6$ in 0.1 M KCl	34
14. Electrochemical impedance spectroscopy of a) CPE, b) $Fe_3O_4/CPE$ , c) $ZrO_2/CPE$ and d) $Fe_3O_4/ZrO_2/CPE$ in 2 mM $K_3Fe(CN)_6$ in 0.1 M KCl	37
15. CVs of 2.5 mM AA a) CPE, b) $Fe_3O_4/CPE$ , c) $ZrO_2/CPE$ and d) $Fe_3O_4/ZrO_2/CPE$ (pH 4, $\nu=100 \text{ mV s}^{-1}$ )	39
16. Cyclic voltammograms of 0.2 M acetate buffer (pH 4) in the absence (a) and presence (b) of 2.5 mM AA at the $Fe_3O_4/ZrO_2/CPE$	40
17. (a) CVs of $Fe_3O_4/ZrO_2/CPE$ in 0.1 M ABS (pH 4) containing 2.5 mM AA at various scan rates; 10, 25, 50, 75 and $100 \text{ mV s}^{-1}$ (b) The plot of anodic peak current vs. square root of the scan rate (c) The plot of log peak current vs. log the scan rate.	41

18. CVs obtained at  $\text{Fe}_3\text{O}_4/\text{ZrO}_2/\text{CPE}$  in 0.2 M ABS in pH values (2, 3, 4, 5 and 6) containing 2.5 mM AA at scan rate  $100 \text{ mV s}^{-1}$ ; c) Variations in the oxidation peak current as a function of pH d) Variations in the oxidation peak potential as a function of pH. 43
19. (a) DPVs of AA on  $\text{Fe}_3\text{O}_4/\text{ZrO}_2/\text{CPE}$  in 0.2 M ABS (pH 4) (b) variations of peak current as a function of AA concentration 44
20.  $\text{Fe}_3\text{O}_4/\text{ZrO}_2/\text{CPE}$  Variation peak current with time in  $2 \mu\text{A}$  AA in 0.2 M ABS (pH 4) 46

## LIST OF TABLES IN THE APPENDIX

<b>Appendix Table</b>	<b>Page</b>
1. Reproducibility $\text{Fe}_3\text{O}_4/\text{ZrO}_2/\text{CPE}$	65
2. Stability $\text{Fe}_3\text{O}_4/\text{ZrO}_2/\text{CPE}$	65

# **Fe<sub>3</sub>O<sub>4</sub>/ZrO<sub>2</sub> Nanocomposite Modified Carbon Paste Electrode; Preparation, Characterization and Application for the Detection of Ascorbic Acid**

## **ABSTRACT**

*Fe<sub>3</sub>O<sub>4</sub>, ZrO<sub>2</sub> and Fe<sub>3</sub>O<sub>4</sub>/ZrO<sub>2</sub> nanocomposites were synthesized by chemical co-precipitation method. The structural and morphological properties of the as-synthesized materials were characterized by FTIR, UV-Vis, XRD and SEM. Results obtained for the nanomaterials confirmed the formation of Fe<sub>3</sub>O<sub>4</sub>, ZrO<sub>2</sub> and Fe<sub>3</sub>O<sub>4</sub>/ZrO<sub>2</sub> nanocomposite. XRD diffraction patterns depicted Fe<sub>3</sub>O<sub>4</sub>, ZrO<sub>2</sub> and Fe<sub>3</sub>O<sub>4</sub>/ZrO<sub>2</sub> crystalline structure and the smaller size of the nanocomposite (9.8 nm) in comparison to the magnetite (52.11 nm) and zirconium oxide (51.5 nm). Electrochemical properties of carbon paste electrode modified by Fe<sub>3</sub>O<sub>4</sub>, ZrO<sub>2</sub> and Fe<sub>3</sub>O<sub>4</sub>/ZrO<sub>2</sub> nanocomposite were studied using cyclic voltammetry (CV) and electrochemical impedance spectroscopy (EIS) in the presence of 2 mM K<sub>3</sub>Fe(CN)<sub>6</sub> and aqueous 0.1 M KCl. The acquired voltammograms demonstrates that Fe<sub>3</sub>O<sub>4</sub>/ZrO<sub>2</sub> nanocomposite showed the highest electrochemical signal compared to the bare CPE and the other modified electrodes. This could be due to the synergistic effect as a result of the high absorption capacity of Fe<sub>3</sub>O<sub>4</sub> and electrocatalytic properties of ZrO<sub>2</sub>. The EIS spectra result was also consistent to that of the CV; CPE modified by the binary system showed a small semicircle (low charge transfer resistance 976 Ω) to that of magnetite 2168 and zirconium oxide 2420 Ω. These behaviors can improve the sensitivity and the response of Fe<sub>3</sub>O<sub>4</sub>/ZrO<sub>2</sub>/CPE proposed sensor for the detection of ascorbic acid (AA). To improve the performance of the sensor pH and scan rate were optimized. Under optimized condition (pH = 4 and  $v = 100 \text{ mV s}^{-1}$ ) Fe<sub>3</sub>O<sub>4</sub>/ZrO<sub>2</sub>/CPE electrode was applied to determine the concentration of AA in standard solution (1 to 6 x 10<sup>-6</sup> M) using differential pulse voltammetry. The sensor exhibits good linear range (1 - 6 μM), sensitivity (11 μA/μM) and detection limit (0.51 μM), reproducibility (2.4 %) and stability (96.91 %). The electrode was also applied to determine AA in paracetamol. The finding demonstrated the developed sensor can be a potential candidate for routine analysis of AA in pharmaceuticals, food and fruit samples.*

**Keywords** - Ascorbic acid, Carbon paste electrode, Magnetite, Nanocomposite, Zirconium oxide

## 1. INTRODUCTION

Ascorbic acid (Vitamin C; found in citrus fruits and vegetable products) is mainly a cure for scurvy, drug poisoning, liver disease, allergic reaction and atherosclerosis (Zhang and Qin, 1996). Besides, ascorbic acid is helpful for building up one's resistance to disease. The body requires ascorbic acid to form collagen protein to maintain bones, blood vessels and skin. It is also added to food as an antioxidant, for stabilization of aroma and colour, as well as to enlarge the life of commercial products. Pharmaceuticals also often contain ascorbic acid as a supplementary source in human diets (Vazquez *et al.*, 2012).

Ascorbic acid (AA) is easily oxidized chemically and electrochemically to L-dehydroascorbic acid (Sabzi and Pournaghi-Azar, 2005). It is unstable, undergoing oxidation, especially in aerobic conditions, alkaline media, and at exposure to light (Zeng *et al.*, 2005). AA is widely found in association with various biologically and pharmacologically active substances, including acetaminophen (Sandulescu *et al.*, 2000) in various pharmaceutical products as well as in biological fluids (Sandulescu *et al.*, 2000; Zhang *et al.*, 2001; Arvand *et al.*, 2003; Ramesh and Sampath, 2004). An overdose amount of AA in some people may lead to diarrhea, nausea, skin irritation and depletion of copper. In addition, AA can cause adverse reactions when taken with some drugs. Therefore monitoring of AA level in the pharmaceutical and in food stuff has become a paramount important.

There are a well-established variety of analytical techniques such as chromatography (Dennison *et al.*, 1981; Lykkesfeldt, 2000), spectrophotometry (Tabata and Morita, 1997; Guclu *et al.*, 2005), mass spectrometry (Conley *et al.*, 2008), flow injection (Alwarthan, 1993; Grudpan *et al.*, 1999), chemiluminescence (Alwarthan, 1993) have been proposed for determination of AA in pharmaceutical preparations, biological fluids, foods and beverages. Besides their valuable characteristics, these techniques require relatively expensive instrumentation, have long times of analysis and require trained personnel.

Electrochemical sensor instruments are portable, compact and inexpensive compared to spectroscopic equipment, critical care, safety issues, and have found wide applications industrial hygiene as well as in process and quality control (Harisha *et al.*, 2015). A very

sensitive, new, versatile and powerful electrochemical voltammetric technique has been successfully used for detection and quantification AA in various samples owing to their high sensitivity, high accuracy, simple operation mode and low cost. However, direct oxidation of AA at bare electrode is irreversible and the subsequent hydrolysis product, 2, 3-diketogluconic acid (Zen *et al.*, 2000), is readily adsorbed onto the electrode surface, which results in electrode fouling with high overpotential, poor reproducibility, low selectivity and sensitivity. In addition, some biological molecules, e.g. dopamine and uric acid, undergo oxidation within the same potential window as AA. To overcome these problems, immobilized surface redox species on the electrode surfaces, namely modified electrodes with carbon nanotubes (Hu *et al.*, 2005), ionic liquid (Zhao *et al.*, 2005), conducting polymers (Manoj *et al.*, 2011), metal nanoparticles (Manoj *et al.*, 2011), metal complexes (Zhang *et al.*, 2012) and polymeric films (Silva *et al.*, 2012) have been employed.

Among conventional electrodes carbon paste electrode (CPE) is one of the most conductive matrixes for preparing chemically modified electrodes (CMEs). Due to their inherent advantages such as very stable electrochemical response, low Ohmic resistance, chemical inertness, easy construction, facile renewability of the surface for electron exchange, long operational lifetime, no need for significant prior pretreatment and suitability for a variety of sensing applications (Svancara *et al.*, 2009). CPEs are nontoxic and environmentally friendly electrodes (Abu-Shawish *et al.*, 2013). The preparation of CPE usually involves the dispersion of graphite powder in a hydrophobic binder to form a homogeneous paste, followed by filling a tube with the resulting paste (Beitollahi *et al.*, 2008, Zhang *et al.*, 2014). The selectivity and sensitivity of the CPEs can be improved by incorporating a selective agent (modifier) in the carbon paste. The modified electrode has good electrocatalytic activity, sensitivity and selectivity; it has also a low detection limit compared to unmodified carbon paste electrodes (Baghayeri and Namadchian, 2013, Beitollahi and Nekooei, 2016).

Metal oxide nanoparticles of a variety of shapes, sizes and compositions exhibit excellent conductivity and fascinating catalytic properties, which make them suitable for constructing novel electrochemical sensors for the determination of AA. Baghizadeh *et al.*, 2015 synthesised ZrO<sub>2</sub>/NPs and modify it with carbon paste electrode for the Determination of AA in presence of Vitamin B<sub>6</sub> in food Samples with their concentration in the ranges of 0.07–850  $\mu$ M AA with

limit of detection  $9 \times 10^{-6}$  M. Nanocomposites can significantly improve the electrocatalytic properties of substrates, decrease the overpotential, increase the reaction rate and improve reproducibility of the electrode response in the area of electroanalysis. Nejad *et al.*, 2016 reported  $\text{Fe}_3\text{O}_4/\text{SiO}_2$  nanocomposite modified carbon paste electrode for voltammetric determination of Ascorbic Acid in the presence of L-Cysteine in the range of  $1.0 \times 10^{-6}$  to  $9.0 \times 10^{-4}$  M ascorbic acid. The limit of detection was equal to  $2.3 \times 10^{-7}$  M. Also Jahani and Beitollahi, 2016 studied  $\text{TiO}_2/\text{Fe}_3\text{O}_4$  nanocomposite modified carbon paste electrode Voltammetric Sensor for Sensitive Ascorbic Acid and Tryptophan Detection 2.5 to  $100.0 \times 10^{-6}$  M. The lower detection limit was found to be  $1.13 \times 10^{-6}$  M for AA. The results indicated that nanocomposites modified electrodes show an enhanced response for the determination of various important biological and clinical species.

To the best of our knowledge there was no report for the detection of AA using  $\text{Fe}_3\text{O}_4/\text{ZrO}_2/\text{CPE}$  nanocomposite. The electrochemical behavior of AA and its detection at the  $\text{Fe}_3\text{O}_4/\text{ZrO}_2$  modified carbon paste electrode surface was studied by differential pulse voltammetry. In addition to this the electrochemical properties of carbon paste modified electrode were also characterized by cyclic voltammetry and electrochemical impedance spectroscopy (EIS).

## **Objectives**

### **General objectives**

To develop a more sensitive  $\text{Fe}_3\text{O}_4/\text{ZrO}_2$  nanocomposite modified carbon paste electrode for the detection of ascorbic acid.

### **Specific objectives**

- To synthesize  $\text{Fe}_3\text{O}_4$ ,  $\text{ZrO}_2$  and  $\text{Fe}_3\text{O}_4/\text{ZrO}_2$  nanocomposites by using co-precipitation method;
- To characterize the morphological and structural properties of  $\text{Fe}_3\text{O}_4$ ,  $\text{ZrO}_2$  and  $\text{Fe}_3\text{O}_4/\text{ZrO}_2$  using FTIR, XRD, UV-Vis and SEM;
- To construct  $\text{Fe}_3\text{O}_4$ ,  $\text{ZrO}_2$  and  $\text{Fe}_3\text{O}_4/\text{ZrO}_2$  nanocomposite modified carbon paste electrode and investigate its electrochemical properties using cyclic voltammetry and electrochemical impedance spectroscopy;

- To optimize experimental parameters such as pH and scan rate of  $\text{Fe}_3\text{O}_4/\text{ZrO}_2$  modified CPE for the determination of ascorbic acid;
- To apply  $\text{Fe}_3\text{O}_4/\text{ZrO}_2/\text{CPE}$  electrode for the detection of ascorbic acid in standard solutions using differential pulse voltammetry (DPV) and
- To apply  $\text{Fe}_3\text{O}_4/\text{ZrO}_2/\text{CPE}$  as electrochemical sensor for the detection of ascorbic acid in paracetamol using DPV.

## 2. LITERATURE REVIEW

### 2.1. Ascorbic Acid

Ascorbic acid (Vitamin C) is a hydrosoluble, antioxidant vitamin, which has a  $\gamma$ -lactone structure, and represents the L-enantiomer of ascorbic acid, the biochemically and physiologically active form. Ascorbic acid is a hexanoic sugar acid with two dissociable protons (pKa 4.04 and 11.34). Therefore, under physiological conditions, it occurs as an ascorbate anion.

Ascorbic acid (AA) is known for its reductive properties, being easily oxidized to dehydroascorbic acid. It acts as a powerful antioxidant which fights against free radical induced diseases (Padayatty *et al.*, 2003). Plants and most animals synthesize ascorbate from glucose. In primitive fish, amphibians and reptiles, ascorbate synthesis takes place in kidney, whereas for mammals liver is the site of synthesis, where the enzyme L-gulonolactone oxidase converts glucose to ascorbic acid Figure 1. Due to a genetic mutation that induce a L-gulonolactone oxidase deficiency, humans, some other primates, and guinea pigs are unable to synthesize ascorbic acid, so they need to take it from diet.

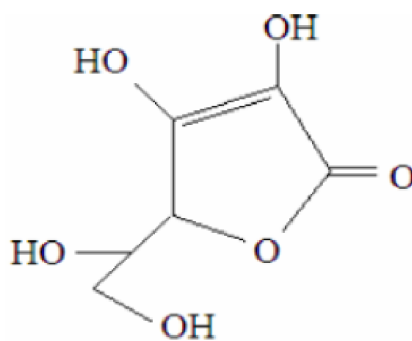


Figure 1. The chemical structure of ascorbic acid

Ascorbic acid can scavenge singlet oxygen, or act as chelating agent. This is claimed as the basis of its ability to protect oxidizable constituents, including phenolic and flavor compounds, therefore being largely used as an antioxidant in foods and drinks. Studies performed on wine showed that the benefit of ascorbic acid as an antioxidant consists in its capacity to scavenge molecular oxygen, before the oxidation of phenolic compounds. Ascorbic acid also appears

to be an ideal free radical scavenger, because it reacts rapidly with hydroxyl (and other) radicals to form relatively unreactive radicals that do not readily propagate (Bradshaw *et al.*, 2011).

Vitamin C can be found in many biological systems and food stuffs, namely fresh vegetables and fruits, as the most ubiquitous water soluble vitamin ever discovered. Rich sources include black-currant, citrus fruit, leafy vegetables, tomatoes, green and red peppers, etc. Vitamin C is involved iron absorption, collagen synthesis and immune response activation and participates in wound healing and osteogenesis, helps maintaining capillaries, bones, and teeth (Padayatty *et al.*, 2003).

Ascorbic acid excess can lead to gastric irritation, and one of its metabolites, oxalic acid, causes renal problems. In some cases, excessive quantities of ascorbic acid may result in the inhibition of natural processes occurring in food and can contribute to taste/aroma deterioration. Another drawback of ascorbic acid excess is its ability to act as a strong antioxidant only in aqueous media and in the absence of heavy metal cations (Bradshaw *et al.*, 2011).

Ascorbic acid is a labile substance as it is easily degraded by enzymes and atmospheric oxygen. Its oxidation is accelerated by excessive heat, light and heavy metal cations. Ascorbic acid is frequently used as an antioxidant in food industry to prevent unwanted changes in color or flavor. As an electron donor, ascorbic acid serves as one of most important small molecular weight antioxidants which contribute to the total antioxidant capacity an important quality indicator of foods and drink. Due to the crucial role of vitamin C in biochemistry and in industrial applications, the determination of vitamin C still presents research interest. Quick monitoring of vitamin C levels during production and quality control stages is important (Pisoschi *et al.*, 2009).

## **2.2. Detection Methods of Ascorbic Acid**

### **2.2.1. Ascorbic Acid Detection by Spectroscopic Techniques**

As the simplest techniques for AA determination could be considered classic titration methods. To the well known and most commonly used oxidant solution used in these determinations belongs 2, 6-dichlorophenol indophenol (DCPIP) (Hughes, 1983), potassium iodate (Deshmukh

and Bapat, 1955) or bromated (Skoog *et al.*, 1998). The main problem of the volumetric methods usage is the lack of specificity. Chromatographic methods, like liquid chromatography (Oliveira and Watson, 2001) and particularly HPLC with electrochemical detection (Rizzolo *et al.*, 2002), have been used in ascorbic acid assessment in food stuffs and biological fluids. Fluorometric methods based on dehydroascorbic acid reaction with o-phenylene diamine and requiring strict control of the pH value (Arya *et al.*, 2000) and UV-VIS absorbance based determinations (Vermeir *et al.*, 2008) were also applied. Ascorbic acid was assessed spectrophotometrically, based on its reaction with hexacyanoferrate (III) (Nobrega and Lopes, 1996), on its oxidation using the Cu (II)-neocuproine complex (Guclu *et al.*, 2005), or on the determination of iodine reacted with ascorbic acid (Danet *et al.*, 1994). Other optical methods for vitamin C estimation include chemiluminescence (Danet *et al.*, 2000).

### **2.2.2. Ascorbic Acid Detection by Electrochemical Techniques**

Ascorbic acid is the most common electroactive biological compound, being easily oxidated, and this constitutes the basis of its electrochemical determination. Ascorbic acid forms with dehydroascorbic acid an irreversible redox couple. Its electrocatalytic oxidation showed only the anodic oxidation peak (Adams *et al.*, 1976 and Wen *et al.*, 1997), for which Randles Sevcik equation described the observed direct dependence between the current intensity corresponding to ascorbic acid electrooxidation and the square root of the potential sweep rate. Regarding ascorbic acid/dehydroascorbic acid redox couple irreversibility, studies have been devoted to the investigation of ascorbic acid oxidation mechanism, which describe an electrochemically reversible electron transfer coupled to irreversible chemical reactions, determining an overall irreversible process: the oxidation of ascorbic acid involves the release of two electrons and two protons, to produce dehydroascorbic acid, which was proved to be followed by an irreversible solvation reaction at pH lower than 4.0.

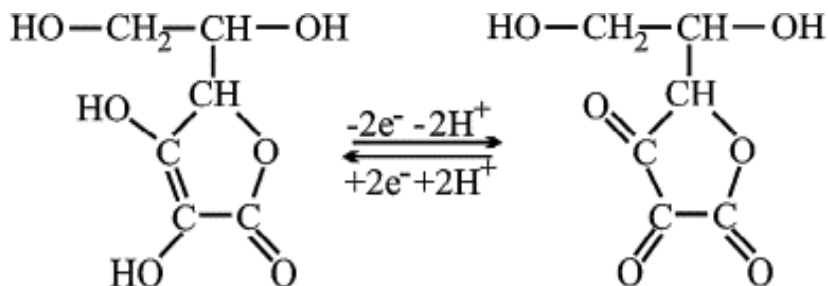


Figure 2. Oxidation of ascorbic acid

This irreversible reaction yields an electroinactive product, 2, 3-diketogulonic acid, formed when dehydro L-ascorbic acid opens its lactone ring, easily adsorbable on the electrode surface, which can result in electrode fouling.

Literature data on ascorbic acid oxidation at  $\text{pH} < 8$  mention two successive one electron oxidation steps accompanied by rapid dehydration rendering the oxidation process irreversible. A detailed description of ascorbic acid oxidation at gold electrode describes two clearly defined stages producing two waves. The first wave is produced by a bi-electronic process in which two protons interchange at the pH range of 2-4.5, one proton at pH 4.5-8 and finally two protons at  $\text{pH} > 8$ . Namely, at pH values inferior to the first pKa value of L-ascorbic acid (approximately 4.5), two protons interchange globally during the process. At higher pH values, a single proton interchanges with ascorbate anion as electroactive species. These considerations are consistent with the variation of the peak potential with pH, observed up to pH 8. It was difficult to identify the products of ascorbic acid oxidation or to carry out a detailed study of the second oxidation wave at pH higher than 8, given the instability of the basic solutions of both L-ascorbic and dehydro-L-ascorbic acids. It was found that the intermediate, ascorbate anion is electrochemically oxidized to a diketolactone, subsequently dehydrated to dehydroascorbic acid which rearranges to another ene-diol further oxidized at higher potentials.

For this irreversible redox couple the anodic peak height correlated with analyte concentration corresponds to the oxidation of the reduced form. Figure 3 shows Cyclic voltammograms obtained with a Pt working electrode for different ascorbic acid concentrations, expressed as mM: 20 (line 1), 15 (2), 10 (3), 5 (4), 2.5 (5), 1.25 (6), 0.625 (7) and 0.31 (8); potential scan rate  $50 \text{ mVs}^{-1}$ ; a  $0.1 \text{ mol L}^{-1}$  KCl solution was used as supporting electrolyte (Pisoschi *et al.*, 2011).

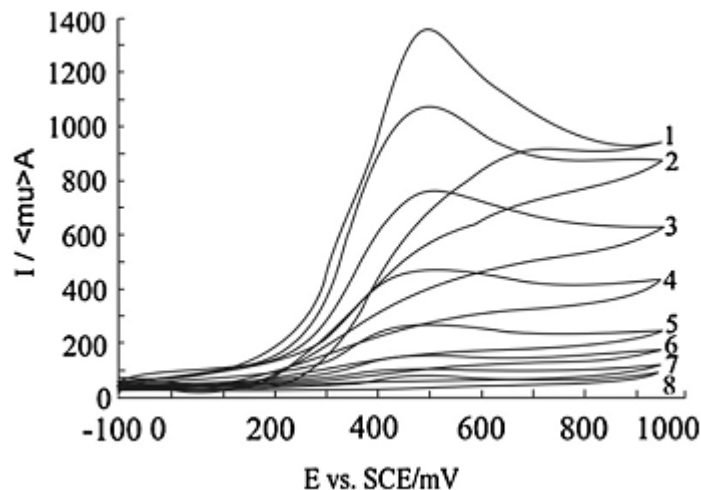


Figure 3. Cyclic voltammograms obtained with a Pt working electrode for different ascorbic acid concentrations

### 2.3. Sensors

Sensors are the devices, which incorporate a recognition element with a signal transducer. Such devices can be used for direct measurement of the analyte in the sample matrix. These devices produce any one of the signals as electrical, thermal or optical output signals which could be converted into digital signals for further processing. One of the ways of classifying sensors is done based on these output signals. Among these, electrochemical sensors have more advantage over the others because; in these, the electrodes can sense the materials which are present within the host without doing any damage to the host system. On the other hand, sensors can be broadly classified into two categories as chemical sensors and biosensors. The biosensors can be defined in terms of sensing aspects, where these sensors can sense biochemical compounds such as biological proteins, nucleotides and even tissues (Wilson and Gifford 2005; Chen and Chzo, 2006). Within these sensors, the active sensing material on the electrode should act as a catalyst and catalyze the reaction of the biochemical compounds to obtain the output signals (Vasantha and Chen, 2006). The combination of these two different ways of classifications has given rise to a new type of sensors which are called electrochemical biosensors, where the electrochemical methods are applied for the construction and working of a biosensor (Zhang *et al.*, 2005).

### 2.3.1. Electrochemical Sensors

Electrochemical sensors (Sun *et al.*, 2013; Yang *et al.*, 2013; Yuan *et al.*, 2014) are subclass of chemical sensors in which the chemical information is transduced into an electrical signal. Electrochemical Sensor is a small device used for direct measurement of a physical quantity of an analyte in a sample matrix. Electrochemical sensor consists of a transduction element covered by a recognition layer which may be chemical or biological materials. The recognition layer interacts with target analyte, and then transduction element translates the chemical changes into electrical signals. Therefore, electrochemical sensor produces an electrical signal that is related to the concentration of an analyte. Electrochemical sensors are especially attractive because of their remarkable delectability, exhibit excellent linearity and repeatability, experimental simplicity and low cost.

### 2.3.2. Amperometric Sensors

Amperometric sensors (Chen *et al.*, 2012; Li *et al.*, 2013; Dalkiran *et al.*, 2014) exploit the use of a potential applied between a reference and a working electrode, to cause the oxidation or reduction of an electroactive species; the resultant current is measured. The instrumentation requires controlled potential equipment and the electrochemical cell, it consists the use of a three electrodes. While the working electrode is the electrode at which the reaction of interest occurs, the reference electrode provides a stable potential compared to the working electrode. An inert conducting material is usually used as auxiliary electrode. A supporting electrolyte is required in controlled potential experiments to eliminate electron migration effects, decrease the resistance of the solution and maintain the ionic strength constant.

### 2.3.3. Conductometric Sensors

Conductometric sensors (Kawakami *et al.*, 2012; soldatkin *et al.*, 2013) measure conductivity at a series of frequencies. Sensors in this group rely on changes of electric conductivity of a film or a bulk material, whose conductivity is affected by the analyte present. Only with the advent of modified surfaces for selectivity and much improved instrumentation have these become more viable methods for designing sensors. There are some practical considerations that make conductimetric methods attractive, such as low cost and simplicity and no reference electrodes

are needed. Electrochemical sensors may also involve capacitative impedance resulting from the polarization of the electrodes and the faradaic or charge transfer processes. Conductance of a homogeneous solution is directly proportional to the cross sectional area perpendicular to the electrical field and inversely proportional to the segment of solution along the electrical field. Thus, the conductance of the solution,  $G$  ( $\Omega^{-1}$ ), can be expressed as equation (i):

$$G = \sigma A/L \quad (i)$$

Where,  $A$  is the cross-sectional area ( $\text{cm}^2$ ),  $L$  is the segment of the solution along the electrical field (cm) and  $\sigma$  ( $\Omega^{-1} \text{cm}^{-1}$ ) is the specific conductivity of the electrolyte and is related quantitatively to the concentration and the magnitude of the charges of the ionic species. For a practical conductivity sensor,  $A$  is the surface of the electrode and  $L$  is the distance between the two electrodes.

## 2.4. Carbon Paste Electrodes

Carbon paste electrodes (CPEs) are among the most popular types of carbon electrodes which have been widely used in electroanalysis, mainly due to such interesting properties as chemical inertness, low cost, wide potential window and suitable for a variety of sensing and detection application. The operational mechanism of the carbon paste electrodes depends on the properties of the modifier materials used to impart selectivity towards the target species (Kalcher *et al.*, 1995; Wang *et al.*, 2000). Carbon paste electrodes (CPEs) have attracted attention as ion selective electrodes mainly due to their advantages over membrane electrodes such as renewability, stable response, low ohmic resistance, no need for internal solution (Javanbakht *et al.*, 2007; Goyal *et al.*, 2008; Wang *et al.*, 2008; Javanbakht *et al.*, 2008).

The carbon paste usually consists of graphite powder dispersed in a non-conductive mineral oil. Carbon paste electrodes (CPEs) are one of the most popular types of carbon electrodes used in electroanalysis, mainly due to that they are inexpensive, easy to prepare and regenerate, they have a wide potential window, low ohmic resistance, low background current, and good selectivity and sensitivity towards target species (Grabecsvogl *et al.*, 1998; Gismera *et al.*, 2004; Svancara *et al.*, 2009). Another advantages of using CPEs include the fact that the operational mechanism of the CPEs depends on the properties of the modifier materials used (Aglan *et al.*,

2012); because of that, the modifier and its interaction with the environment, can be studied by electrochemical techniques using modified carbon paste electrodes (MCPEs); followed later by SEM-EDS in order to complement the studies of the metals reactions that were carried out on the surface of the CPEs due to the presence of metallic films plated onto the carbon paste surface. However, the inherent disadvantages of CPEs such as low mechanical stability and reproducibility limit their practical application. Moreover, the use of nonconductive binders such as paraffin oil may weaken the electrochemical performance of CPEs (Kadara *et al.*, 2009). The advantages and disadvantages of CPE are summarized in Table 2.

Table 1. Advantages and Limitation of Carbon Paste Electrode

Advantage	Limitation
Easily obtained at minimal cost	Depends on experience of the user
Highly sensitive sensors for both inorganic and organic electrochemistry	Each probe must be calibrated individually The transfer rate is slower compared to that of metal electrode
Easy to use, good sensitivity and non toxic	
Has wide potential window and long time stability	Low mechanical stability and reproducibility limit their application
Low Ohmic resistance (less than 10 ohm)	
Experimental works with CPEs are very convenient	

## 2.5. Chemically Modified Carbon Paste Electrode

A chemically modified Carbon paste electrode (CMCPE) is an electrical conductor that has its surface modified for different electrochemical functions. The area of surface modified electrodes is of particular interest because of its application in sensors. Such modifications in the electrode surface lead to greater control on the reactivity at the interface. The distinguishing feature of a CME is that a thin film of a selected material is coated on the surface of electrode to endow the electrode with the chemical, electrochemical, optical, electrical and other desirable properties of the film. The use of both carbon paste electrodes (CPEs) and chemically modified carbon paste

electrodes (CMCPEs) may result in very sensitive and promising analytical method (Wang *et al.*, 1995; Fernandez-Sanchez and Costa-Garcia, 1997).

Chemically modified carbon paste electrodes (CMCPEs) are especially useful in the determination of traces of metal species and organic compounds. The analyte is first bound at the electrode surface via a non-electrochemical interaction with the embedded modifier, e.g. chemical reaction or adsorption process, so that a sensitive and/or a selective accumulation are achieved. Usually modifiers for the determination of metal cations are crown ethers (Prabhu *et al.*, 1989), ion exchangers (Agraz *et al.*, 1991), organic polymers complexing agents (Lu *et al.*, 2000, Mousavi *et al.*, 2001, Svancara *et al.*, 2001), or minerals (Kula, 1999 and Navratilova, 2000). Normally the modifier is directly embedded in the paste of the electrode, which consists of a homogeneous mixture of graphite and nujol (Kalcher *et al.*, 1995). The development and application of chemically modified carbon paste electrodes (CMCPEs) have received considerable attention in recent years because they have advantages of cheap, simple manufacture, wider operational potential window, renewable surface, high stability, and sensitivity (Kamyabi and Aghajanloo, 2008). The incorporation of electroactive materials into a carbon paste electrode is advantageous and has been widely applied in the electroanalytical community. One of the most important effects of modifier is decreasing the redox potential required for the electrochemical reaction and enhancing the sensitivity and selectivity of the detection method (Shahrokhian *et al.*, 2004).

## 2.6. Nanoparticle

Nanoparticles which in general terms are defined as engineered structures with diameters of less than 100 nm are devices and systems produced by chemical and/or physical processes having specific properties (Maureen and Val-Vallyathan, 2006). The reason why nanoparticles are attractive for such purposes is based on their important and unique features, such as their surface to mass ratio, which is much larger than that of other particles and materials, allowing for catalytic promotion of reactions, as well as their ability to adsorb and carry other compounds. The reactivity of the surface originates from quantum phenomena and can make NP unpredictable since, immediately after generation, NPs may have their surface modified,

depending on the presence of reactants and adsorbing compounds, which may instantaneously change with changing compounds and thermodynamic conditions.

Materials in micrometer scale mostly exhibit physical properties the same as that of bulk form but materials in the nanometer scale exhibit properties distinctively different from that of bulk due to quantum size effects and the occurrence of large amounts of surfaces and interfaces because of their reduced size in nanometer scale (Ventra *et al.*, 2004). And thus the materials having three dimensional network consisting of at least two phases with one dispersed in another i.e., matrix are known as nanocomposites. Mixing of two or more dissimilar nanomaterials coated on the electrode surface called nanocomposite. It has unique physical, electrical, optical and chemical properties. The major advantages of the composite electrode materials are to enhance the electroactive surface and good electrical contact between components and transducers (Fang *et al.*, 2012).

## **2.7. Metal Oxide Nanoparticles**

Transition metal oxides have many applications as catalysts (Bennici *et al.*, 2003; Xu *et al.*, 2003; Altinc *et al.*, 2008; Lu *et al.*, 2008; Lv *et al.*, 2008), sensors (An *et al.*, 2008; Yang *et al.*, 2011), superconductors (Pillai *et al.*, 1995; Wu *et al.*, 2003) and adsorbents (Zou *et al.*, 2006; Wei *et al.*, 2010; Han *et al.*, 2009). Metal oxides constitute an important class of materials that are involved in environmental science, electrochemistry, biology, chemical sensors, magnetism, and other fields. One of their most important applications is heterogeneous catalysis. Iron oxides belong to the most abundant minerals and occur with a large variety of stoichiometries, structures, and properties. Mixing of two or more dissimilar nanomaterial's coated on the electrode surface called nanocomposite. It has unique physical, electrical, optical and chemical properties. The major advantages of the composite electrode materials are to enhance the electro active surface and good electrical contact between components and transducers (Fang *et al.*, 2012). Synthesis of various functional nanomaterials such as metals, semiconductors, magnetic materials and so forth has been of immense scientific and technological interest (Ge *et al.*, 2009).

### **2.7.1. Carbon Material Based Electrochemical Sensors**

Carbon material based electrochemical sensors have been employed for the detection of various analytes with rapid electron transfer kinetics. Based on the remarkable properties of carbon nanomaterials; like graphene, reduced graphene oxide, carbon nanotubes, graphite and graphene oxides which also include large surface area, mechanical, superior electrical and thermal properties, enhance electron transfer, and promote adsorption of molecules. All these are excellent materials in different application area (Pumer *et al.*, 2010). At present, various spectroscopic graphites suitable for the preparation of carbon pastes are available. Graphites and glassy carbon powders are also of a very good quality. The carbon paste usually consists of graphite powder dispersed in a non-conductive mineral oil. The above mentioned carbon powders are characterized by a high uniformity of particle size distribution, high purity, and more or less suppressed sorption capabilities. These characteristics are principally important for the preparation of carbon pastes which are to be used in the current measurement-based techniques such as voltammetry, coulometry or amperometry (Kalcher *et al.*, 1995).

## **2.8. Synthesis Techniques of Nanocomposite**

### **2.8.1. Co-Precipitation Method**

The co-precipitation method involves the separation of solid containing target metal ions from a solution phase. In the process of co-precipitation, the metal components of the super conducting materials are first dissolved in solution. The solution combines with the precipitants in the supersaturated condition to form ion associates or clusters. A homogeneous co-precipitation process results in the formation of crystalline or amorphous solids which depends upon the condition under which the precipitate has been formed, the individual characteristics of the particular substance and its aging after precipitation. The most important advantage of this technique is its feasibility for large-scale production as well as its simplicity and low cost (Wang *et al.*, 2010). Co precipitation method also offers some other advantages: simple and rapid preparation, easy control of particle size and composition, various possibilities to modify the particle surface state and overall homogeneity, homogeneity in mixed precipitates and high specific surface of the products (Pradhan *et al.*, 2001).

### **2.8.2. Sol-Gel Method**

The sol-gel process is a capable wet chemical process to make ceramic and glass materials. This synthesis technique involves the conversion of a system from a colloidal liquid, named sol, into a semi-solid gel phase (Brinker *et al.*, 1988; Jones, 1989; Brinker and Scherer, 1990). The sol-gel technology can be used to prepare ceramic or glass materials in a wide variety of forms: ultra-fine or spherical shaped powders, thin film coatings, ceramic fibres, microporous inorganic membranes, monolithics, or extremely porous aerogels. This technique offers many advantages including the low processing temperature, the ability to control the composition on molecular scale and the porosity to obtain high surface area materials, the homogeneity of the final product up to atomic scale.

### **2.8.3. Hydrothermal Method**

Hydrothermal synthesis is typically carried out in a pressurized vessel called an autoclave with the reaction in aqueous solution (Chen and Mao, 2007). The temperature in the autoclave can be raised above the boiling point of water, reaching the pressure of vapour saturation. Hydrothermal synthesis is widely used for the preparation of metal oxide nanoparticles which can be easily obtained through hydrothermal treatment of peptized precipitates of a metal precursor with water (Yang *et al.*, 2001; Chen and Mao, 2007). The hydrothermal method can be useful to control grain size, particle morphology, crystalline phase and surface chemistry through regulation of the solution composition, reaction temperature, pressure, solvent properties, additives and aging time (Carp *et al.*, 2004).

## **2.9. Electrochemical Characterization**

### **2.9.1. Cyclic Voltammetry (CV)**

Cyclic voltammetry (CV) is one of the simple and popularly used electrochemical techniques. The technique is used as a preliminary step to determine the redox processes in a given analyte (Astruc, 2004). These include, but not limited to the redox potentials, kinetics of an electron transport process and the number of electrons transferred by a material immobilised on the surface of an electrode or in a solution during an electrochemical reaction (Mabbott, 1983).

A typical CV experimental set-up consists of three electrodes; working, reference and counter electrode which are connected to a potentiostat. The potentiostat is used to control the potential on the counter electrode versus the working electrode so that the potential difference between the working and reference electrode is well defined and corresponds to the specified values (PGSTAT, 2011). During the experiment, a potential is applied on the working electrode and is varied from an initial value ( $E_i$ ) to a final value  $E_f$ , (also known as a switching potential) at a constant scan rate leading to a single linear sweep. Once the  $E_f$  is reached, the potential can be reversed back to the  $E_i$  while maintaining the same scan rate to complete a cycle which consists of the forward and reverse sweeps (Zanello, 2007), as indicated in Figure 4.

These cycles can be repeated several times depending on the type of information needed by the analyst. As the potential is cycled (scanned back and forth) within a selected potential window the material will undergo either oxidation or reduction depending on the direction of the potential. When the scan is initiated from the negative potential to the positive potential the analyte will undergo oxidation. This is the region where the analyte's anodic peak current ( $I_{p,a}$ ) and potential ( $E_{p,a}$ ) are observed. The reverse scan will lead to the reduction of the analyte which is defined by the cathodic peak current ( $I_{p,c}$ ) and potential ( $E_{p,c}$ ) (Mabbott, 1983; Monk, 2008).

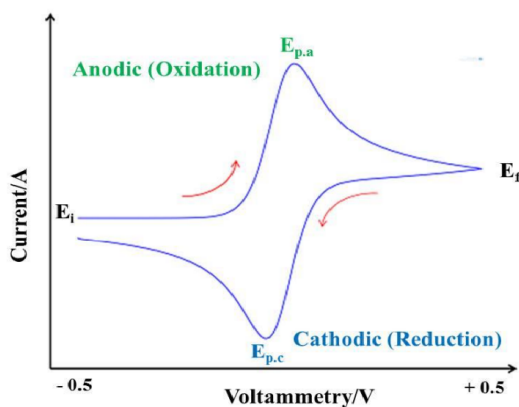


Figure 4. A typical cyclic voltammogram depicting oxidation and reduction peaks of an analyte between specified values of  $E_i$  and  $E_f$  (in this case -0.5 to 0.5 V).

There are several parameters that can be used to determine the reversibility of a given system. Reversibility refers to how fast a reaction can maintain the concentration of oxidised and reduced species in equilibrium at the surface of the electrode. One of these parameters is the formal

reduction potential and is obtained by taking the average of the forward and reverse potentials from the cyclic voltammograms (Mabbott, 1983), as defined by Equation 2.

$$E^{\circ} = \frac{(E_{pa} + E_{pc})}{2} \quad (\text{ii})$$

Cyclic voltammograms can assume various shapes due to the nature of different redox processes of an analyte on the surface of the electrode. The shape of these curves Figure 5 is associated with the reversibility of the electrochemical process on the surface of an electrode.

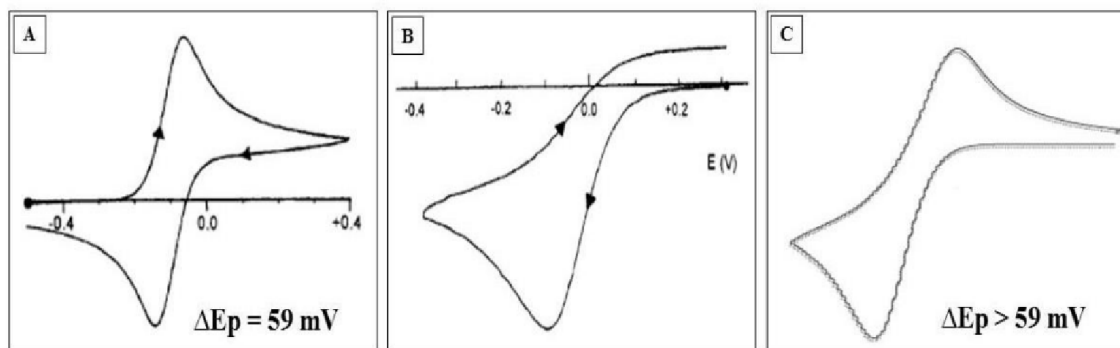


Figure 5. Cyclic voltammetry profiles for (A) reversible, (B) irreversible and (C) quasireversible processes.

A reversible process is characterized by the shape of the cyclic voltammogram represented in Figure 5A. The anodic peak is the mirror image of the cathodic peak. Such electrode processes are classified to be reversible because the rate of the electron transfer is greater than the rate of the mass transport when an electrode is placed inside an electrolyte solution. In cases where the electron transfer is less than that of the mass transport, then that process is defined as irreversible as indicated by Figure 5B. In such processes the peak-to-peak separation is very large and only the reduction peak is detected. In a quasireversible process Figure 5C, the electrode processes show a reversible behaviour at low scan rates, however it becomes irreversible at high scan rates (Zanello, 2007).

### 2.9.2. Electrochemical Impedance Spectroscopy (EIS)

Electrochemical Impedance Spectroscopy (EIS) is an effective tool for studying and monitoring the functioning of batteries and fuel cells. It is also used in other application such as corrosion

analysis and interfacial behaviour of different electrode systems (Randviir and Banks, 2013). Voltammetric techniques are used as a primary step to study the kinetics of an electrode process. However, their results are usually clouded by side effects such as the ohmic drop related to the experimental set-up or the charging currents of the double layer that occurs over a very short time-scale (order of millisecond). The problem with these side effects, more especially ohmic drop, is that the response of a reversible system becomes similar to that of a kinetically slow system. The best way to differentiate the kinetics of these reactions is to make use of an excitation function that will cover a large time domain (Girault, 2004). In that way, EIS studies will be a complement to whatever that is obtained using voltammetric techniques and better explains the kinetics of an electrode process.

EIS experiments are performed by applying a sinusoidal voltage using a potentiostat across a three electrode cell containing an electrolyte solution to retain the analyte of interest. The amplitude and magnitude of the fixed sinusoidal voltage is varied depending on the needs of the user. For example, biological molecules are usually subjected to low voltages to avoid denaturing, whereas this is not the case for non-biological molecules. When the voltage is applied on the electrode in a particular frequency range, current flows through the electrochemical cell and this response is recorded by the potentiostat and converted into impedance data which contains both real and imaginary component (Randviir and Banks, 2013). The obtained data requires a complex process of analysing which can be achieved by using designated EIS analysis software. An electrochemical cell is represented using an equivalent circuit of resistors and capacitors before analysis with the software (Bard *et al.*, 1980). The analysed data is usually presented in the form of a Nyquist plot or Bode plot, as shown by Figure 6.

The Nyquist plot displays real impedance ( $Z'$ ) vs imaginary impedance ( $Z''$ ) and is used to determine the solution resistance ( $R_s$ ), charge transfer resistance ( $R_{ct}$ ) and the Warburg element ( $W_o$ ) of an electrochemical reaction on the electrode surface. This type of plot gives insights about the electrochemical reactions on the surface of the electrode and describes whether they occur via a kinetic or mass transfer controlled processes. The determining feature between the two processes is  $R_{ct}$  and will be large for an electrochemical system governed by kinetically controlled, whereas a significantly small  $R_{ct}$  value will be obtained for mass transfer controlled

systems (Bard, 1980). In addition, there is also a Bode plot which can be used to determine the capacitive or inductive effect of an electrochemical system (Randviir and Banks, 2013). This is a plot of impedance and phase angle against frequency as shown in Figure 6B.

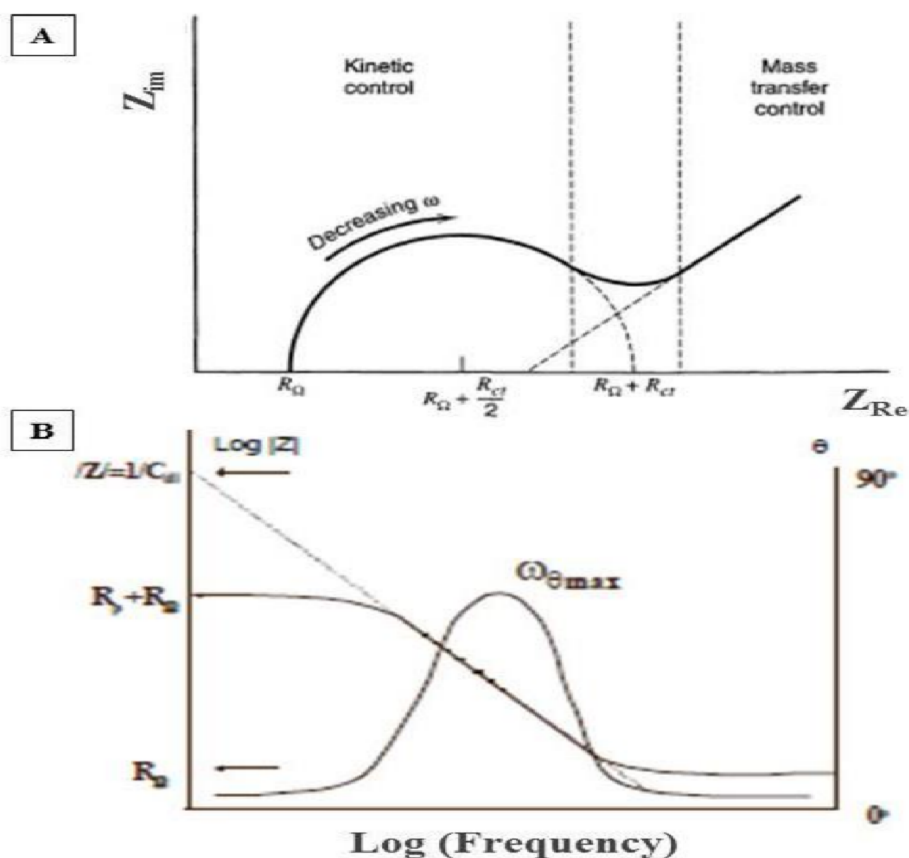


Figure 6. Electrochemical impedance depicted by (A) the Nyquist plot (Bard et al., 1980) and (B) Bode plot (Anonymous, n.d.)

### 2.9.3. Differential Pulse Voltammetry (DPV)

The basis of all pulse techniques is the difference in the rate of decay of background and faradaic currents following a potential step. The background current decays exponentially, whereas the faradaic current decays as a function of  $1/(\text{time})^{1/2}$ ; that is, the rate of decay of the background current is considerably faster than the decay of the faradaic current. The background current is negligible at a time of  $5\tau_{\text{RuCdl}}$  after the potential step ( $\tau_{\text{RuCdl}}$  is the time constant for a given electrochemical cell, and ranges from  $\mu\text{s}$  to  $\text{ms}$ ). Therefore, after this time, the measured current

consists solely of the faradaic current; that is, measuring the current at the end of the potential pulse allows discrimination between the faradaic and charging current.

Differential pulse voltammetry (DPV) is comparable to normal pulse voltammetry in that the potential is also scanned with a series of pulses. However, it differs from NPV because each potential pulse is fixed, of small amplitude (10 to 100 mV), and is superimposed on a slowly changing base potential. Current is measured at two points for each pulse, (i) just before the application of the pulse, and the second (ii) at the end of the pulse. These sampling points are selected to allow for the decay of the non-faradaic current. The difference between current measurements at these points for each pulse is determined and plotted against the base potential.

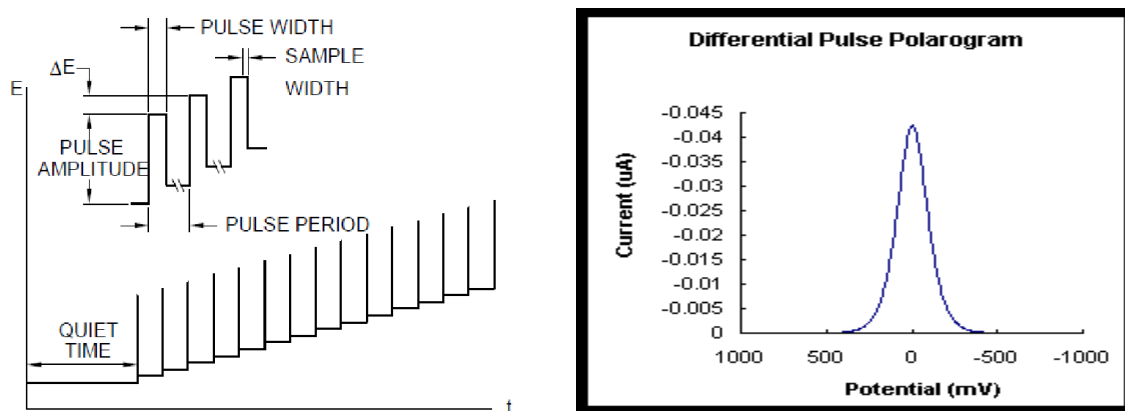


Figure 7. Potential wave form and response for DPV

### 3. MATERIALS AND METHODS

#### 3.1. Experimental Sites

Synthesis of  $\text{Fe}_3\text{O}_4$ ,  $\text{ZrO}_2$  and  $\text{Fe}_3\text{O}_4/\text{ZrO}_2$  nanocomposite, preparation of  $\text{Fe}_3\text{O}_4$ ,  $\text{ZrO}_2$  and  $\text{Fe}_3\text{O}_4/\text{ZrO}_2$  nanocomposite MCPEs, Uv-Vis characterization for synthesized nanocomposites and CV, DPV and EIS electrochemical characterization of the modified electrodes were conducted at the research laboratory of Chemistry Department, Haramaya University. XRD characterization and FT-IR analysis of  $\text{Fe}_3\text{O}_4$ ,  $\text{ZrO}_2$  and  $\text{Fe}_3\text{O}_4/\text{ZrO}_2$  nanocomposite were conducted at Addis Ababa University. Morphological size of nanocomposites by SEM was characterized at the Spanish National Research Council (CSIC) in Madrid, Spain.

#### 3.2. Instruments and Apparatus

X-ray diffractometer (XRD) (BRUKER D8 Advanced XRD), Uv-Vis spectrophotometer (SANYO, SP65) and SEM (JEOL JSM848) were used for morphological and structural analysis of the as synthesized nanocomposite. FTIR spectra were recorded by using spectrophotometer. Bioanalytical systems (BAS 100B) Electrochemical analyzer in three electrode system with  $\text{Fe}_3\text{O}_4$ ,  $\text{ZrO}_2$  and  $\text{Fe}_3\text{O}_4/\text{ZrO}_2$  MCPE, platinum wire and silver/silver chloride ( $\text{Ag}/\text{AgCl}$  3 M KCl) as working, counter and reference electrode, respectively, was used to study the electrochemical behavior of the MCPE using cyclic voltammetry, impedance spectroscopy and differential pulse voltammetry. Plastic tube of 3 mm internal diameter and 6 cm length, an agate mortar and pestle, copper wire, polishing paper, analytical balance, spoon, magnetic stirrer, crucible, thermometer, volumetric flasks (10, 50, 100, 250, 500 mL), analytical balance, 10 mL pipette, measuring cylinder (10, 50, 100, 200, 250, 500 mL), Whiteman No.42 (125 mm) filter paper, pH meter (pH-016), micropipettes (20  $\mu\text{L}$ ), conical flasks and beakers of various size, plate and stirrer for heating were used during this study.

#### 3.3. Chemicals and Reagent

Ferric chloride hexahydrate ( $\text{FeCl}_3 \cdot 6\text{H}_2\text{O}$ , 99%), ferrous chloride tetrahydrate ( $\text{FeCl}_2 \cdot 4\text{H}_2\text{O}$ , 99%), zirconium oxychloride octahydrate salt ( $\text{ZrOCl}_2 \cdot 8\text{H}_2\text{O}$ ,  $\geq 95.5\%$ ), benzene dicarboxylic acid ( $\text{H}_2\text{BDC}$ , 98%), Dimethyl formamide, methanol (98%), KCl (Merck, Germany), nitrogen

gas, and  $\text{K}_3\text{Fe}(\text{CN})_6$  (95%, Merck, Germany) (99 %)  $\text{CH}_3\text{COOH}$  (99.9 %, Sigma Aldrich, Germany),  $\text{CH}_3\text{COONa}$ , (98 %, BDH, England),  $\text{NaOH}$  (99 %, Sigma Aldrich, Germany),  $\text{HCl}$  (37 %, Sigma Aldrich, Germany) were purchased from Aldrich and used as received. Ascorbic acid tablet dosage forms were bought from the local market. Double distilled water was used throughout for the preparation of solutions in all experiments. 95 % graphite (Merch Millipore, Germany) and 98 % Paraffin (Merch, Mumbai) was used for the preparation of carbon paste electrode.

### **3.4. Procedures for the Synthesis of Nanomaterials**

#### **3.4.1. Synthesis of $\text{Fe}_3\text{O}_4$ Nanoparticles**

The magnetite nanoparticle was prepared by chemical co-precipitation method as reported by (Fekadu, 2016). In the first step, stoichiometrically calculated  $\text{FeCl}_2 \cdot 4\text{H}_2\text{O}$  and  $\text{FeCl}_3 \cdot 6\text{H}_2\text{O}$  were accurately weighed and the calculated amounts were dissolved in 100 mL of 0.3 M  $\text{HCl}$  solution. Then, the solution was added drop wise from separatory funnel into 120 mL of 3 M  $\text{NaOH}$  aqueous solution over period of 2 h, under vigorous stirring at 80 °C in  $\text{N}_2$  atmosphere. During this process, the pH of mixture was kept at 12 using 0.1, 0.01 and 0.001 M  $\text{NaOH}$  or  $\text{HNO}_3$  solutions. The suspension was undisturbed for 4 h to form the solid phase at the bottom. The settled phase was washed with deionized water several times to obtain a suspension of  $\text{Fe}_3\text{O}_4$  and then dried at 60 °C for 24 h to obtain the desired product.

#### **3.4.2. Synthesis of $\text{ZrO}_2$ Nanoparticles**

Zirconium oxychloride octahydrate salt ( $\text{ZrOCl}_2 \cdot 8\text{H}_2\text{O}$ ) 3.94 g was dissolved in 50 mL of DMF and stirred for 30 min. In a separate volumetric flask 2.06 g of benzene dicarboxylic acid ( $\text{H}_2\text{BDC}$ ) was dissolved in 50 mL of DMF and stirred for 30 min. Then the metal salt solution was added to the linker solution slowly. These samples were placed in an oven set at a temperature of 120 °C to continue the reaction for 24 h. The precipitate formed after centrifugation at 2500 rpm for 30 min. The precipitate was washed three times with DMF and three times with methanol successfully to remove impurities. The solid obtained as such was dried overnight in open air at room temperature (Silva *et al.*, 2010) and then calcined at 500 °C for 6 h resulting in  $\text{ZrO}_2$  nanoparticles.

### 3.4.3. Synthesis of Fe<sub>3</sub>O<sub>4</sub>/ZrO<sub>2</sub> Nanocomposite

The Fe<sub>3</sub>O<sub>4</sub>/ZrO<sub>2</sub> nanocomposite was prepared by chemical co-precipitation method as reported by (Fekadu, 2016) with a synthesis protocol composition of Fe<sub>3</sub>O<sub>4</sub>/ZrO<sub>2</sub> with Fe:Zr mole ratio of 75:25. It was prepared by weighing FeCl<sub>3</sub>.6H<sub>2</sub>O (8.1 g), FeCl<sub>2</sub>.4H<sub>2</sub>O (3 g) and ZrOCl<sub>2</sub>.8H<sub>2</sub>O (1.6 g). The magnetite–zirconia oxide nanocomposite of each sample was prepared by adding 100 mL of ZrOCl<sub>2</sub>.8H<sub>2</sub>O dissolving in 100 mL of deionized water into the obtained Fe<sub>3</sub>O<sub>4</sub> suspension and ultrasonicated for 10 min prior to use. The pH of the mixtures was adjusted to 8 using 0.1, 0.01 and 0.001 M NaOH and HCl. Then the mixture was magnetically stirred under N<sub>2</sub> atmosphere for 1.5 h at 70 °C. Finally the resulting magnetic compound was separated by permanent magnet and washed with deionized water several times to remove impurities such as Cl<sup>-</sup>, NO<sub>3</sub><sup>-</sup> and excess OH<sup>-</sup> ions and then dried at 60 °C for 24 h to obtain the desired products.

### 3.4.4. Preparation of Carbon Paste Electrode

5 gm of Graphite powder and 1.8 mL of paraffin (4:1 w/w ratios) were measured and mixed together in a mortar and pestle to get the blend and were mixed for 30 minutes until a homogeneous paste was obtained. The prepared homogenized paste was taken and kept in a plastic tube (inner diameter of 3 mm and length of 6 cm) and then a copper wire was inserted to provide electrical contact. The surface of the electrode was polished with a weighing paper until it had a shiny appearance before utilization (Tesfaye *et al.*, 2016).

### 3.4.5. Preparation of Fe<sub>3</sub>O<sub>4</sub>, ZrO<sub>2</sub> and Fe<sub>3</sub>O<sub>4</sub>/ZrO<sub>2</sub> nanocomposite Modified Carbon Paste Electrode

The modified carbon paste electrode was prepared by mixing of 2.01 g graphite, Fe<sub>3</sub>O<sub>4</sub>, ZrO<sub>2</sub> and Fe<sub>3</sub>O<sub>4</sub>/ZrO<sub>2</sub> nanocomposite 0.39 g each and 0.6 g of paraffin oil. Then, the mixture was mixed well for 50 min until a uniformly wetted paste was obtained. The prepared homogenized paste was taken and kept in glass tube (inner diameter of 3 mm and length of 6 cm) and then a copper wire was inserted to provide electrical contact.

### 3.5. Preparation of Acetate Buffer Solutions

The 0.2 M acetate buffer was prepared by weighing approximately 8.2 g of  $\text{CH}_3\text{COONa}$  and 5.7 mL of  $\text{CH}_3\text{COOH}$  and mixing into a 500 mL volumetric flask. The desired pH (2 to 5) of the buffer solution was adjusted with 0.2 M  $\text{CH}_3\text{COOH}$  or 0.2 M  $\text{NaOH}$ . All the prepared buffer solutions were stored in a refrigerator at 4 °C.

### 3.6. Electrochemical Characterization of Nanocomposites

Carbon pastes and modified carbon pastes electrodes, potential windows were established at 100 mV/s scan rate in aqueous  $\text{KCl}$  (0.1 M) and characterized by cyclic voltammetry with potential scanning between -200 mV to + 600 mV vs.  $\text{Ag}/\text{AgCl}$  at different scan rates: 10, 25, 50, 75 and 100  $\text{mVs}^{-1}$ . EIS was performed in 0.1 M  $\text{KCl}$  containing 2 mM  $\text{K}_3[\text{Fe}(\text{CN})_6]$  in the frequency range of 1 Hz-100 kHz at an amplitude of 10 mV. Stock solution of AA was freshly prepared prior to use. Its electrochemical experiments were carried out in a 0.1 M acetate buffer solutions (ABS pH = 3.5). Finally, the differential pulse voltammograms (pulse potential of 50.0 mV, pulse duration of 50.0 ms and pulse period of 0.2 s) were recorded from 1  $\mu\text{M}$  - 6  $\mu\text{M}$ . All measurements were carried out at room temperature.

### 3.7. Spectroscopic Characterization

The FTIR spectrum of the as-synthesized nanocomposites was determined using the  $\text{KBr}$  disc method. The IR absorption pattern was recorded between 400 and 4000  $\text{cm}^{-1}$  using SHIMADZU (1730, Japan) spectrometer. Powder X-ray diffraction pattern was recorded with X'Pert Pro PANalytical with  $\text{CuK}\alpha$  radiation ( $\lambda = 1.5405 \text{ \AA}$ ). The morphology and particle size distribution of the solids were determined by scanning electron microscopy (SEM) using a Hitachi TM1000 with EDX detector. For the estimation of nanocomposites characteristic maximum absorption of  $\text{Fe}_3\text{O}_4$ ,  $\text{ZrO}_2$  and  $\text{Fe}_3\text{O}_4/\text{ZrO}_2$  samples with UV-Vis absorption were measured using SANYO, SP65 spectrophotometer by scanning over 200-800 nm wavelength.

### 3.8. Optimization of Experimental Parameters

#### 3.8.1. Influence of pH

Voltammetric response of ascorbic acid at a surface of Fe<sub>3</sub>O<sub>4</sub>/ZrO<sub>2</sub>/CPE was carried out in pH range 2-6 acetate buffers solutions. Oxidation peak current of AA was investigated using cyclic voltammetry.

#### 3.8.2. Influence of Concentration

Differential pulse voltammetry was used to study the concentration effect of AA by varying from  $1 \times 10^{-6}$  to  $6 \times 10^{-6}$  M at the Fe<sub>3</sub>O<sub>4</sub>/ZrO<sub>2</sub>/CPE in 0.2 M acetate buffer solution at pH 4.

### 3.9. Determination of Ascorbic Acid

Five Vitamin C effervescent tablets (labeled 500 mg per tablet, Hakim Pharmaceutical Company, Iran) were ground. Then, the tablet solution was prepared by dissolving 1.07 g of the powder in 25 mL water by ultrasonication. The contents of the flask were centrifuged for 15 min at 4000 rpm to complete dissolution. Then, different volume of the diluted solution was transferred into a 25 mL volumetric flask and diluted to the mark with acetate buffer solution. The solution was kept in a refrigerator at 4 °C. The content of Vitamin C in standard addition was determined using the various MCPE (Jahani and Beitollahi, 2016). Each solution was transferred into the voltammetric cell. Before the experiment the solutions were deaerated with nitrogen gas (analytically pure with 99.99 %) for 5 min to remove dissolved oxygen.

### 3.10. Method Detection Limit

Detection limit is the lowest concentration level that can be determined at 95 % confidence (Polkowska *et al.*, 2000) or minimum concentration that can be detected by the analytical method with a given certainty a general accepted definition of detection limit is the concentration that gives a signal three times the standard deviation of the blank or background signal (Tuzen *et al.*, 2004).

$$\text{LOD} = 3 \times \sigma / m \quad (\text{iii})$$

Where  $\sigma$  stands standard deviation and  $m$  stands slope of the graph

## 4. RESULTS AND DISCUSSION

### 4.1. Structural and Morphological Characterization of as Produced Nanomaterials

#### 4.1.1. XRD Analysis

Figure 8. shows the XRD pattern of  $\text{Fe}_3\text{O}_4$ ,  $\text{ZrO}_2$  and  $\text{Fe}_3\text{O}_4/\text{ZrO}_2$  nanocomposite. The sharp diffraction peaks are a clear indication that the powders have a crystalline structure. The diffraction peaks for the as-formed sample at  $2\theta = 28^\circ, 30.60^\circ, 35.5^\circ, 45^\circ, 50.2^\circ$  and  $60.3^\circ$  correspond to the phases of  $\text{ZrO}_2$ . At angle  $30.60^\circ$  highly crystalline peak was revealed. The diffraction peaks at  $2\theta = 35.42^\circ$  could be indexed to magnetite. At angle  $30.26^\circ$  the major peak was observed for  $\text{Fe}_3\text{O}_4$  and  $\text{ZrO}_2$  interaction.

The average crystalline size of the nanocomposite can be calculated by using Debye-Scherrer Equation.

$$D(\text{nm}) = \frac{k\lambda}{\beta \cos \theta} \quad (\text{iv})$$

Where, D is crystallite size in nm, k Scherrer constant (0.89),  $\beta$  is the full-width-at-half-maximum (FWHM) of the reflected XRD peak in radians,  $\lambda$  is wavelength of X-ray (1.5406 Å = 0.15406 nm), and  $\theta$  half diffraction angle of peak (in degree). The crystallite size of the  $\text{Fe}_3\text{O}_4$ ,  $\text{ZrO}_2$  and  $\text{Fe}_3\text{O}_4/\text{ZrO}_2$  nanocomposite were 52.11, 51.5 and 9.8 nm respectively. From this result,  $\text{Fe}_3\text{O}_4/\text{ZrO}_2$  nanocomposite has small particle size as well large surface area so it is better to sensor application.

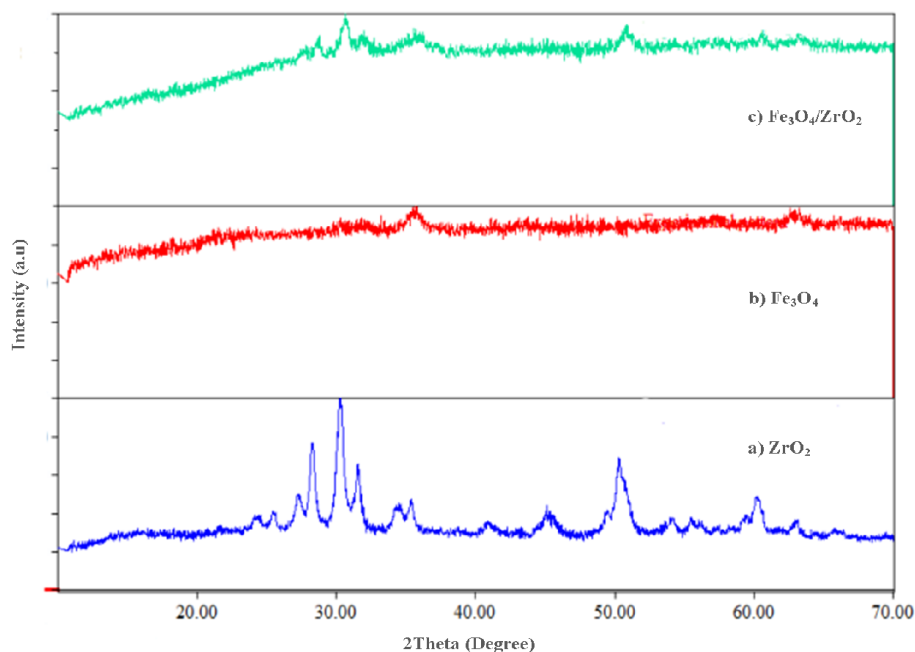


Figure 8. XRD pattern of (a)  $ZrO_2$ , (b)  $Fe_3O_4$  nanoparticles and (c)  $Fe_3O_4/ZrO_2$  nanocomposite

#### 4.1.2. Scanning Electron Microscopy (SEM)

The morphology and elemental composition of  $ZrO_2$ ,  $Fe_3O_4$  and  $ZrO_2/Fe_3O_4$  nanocomposites were characterized by SEM-EDX.  $ZrO_2/Fe_3O_4$  nanocomposites Figure 9 has no distinct morphology but there is aggregation of irregular shaped nanoparticle of various sizes and EDX analysis of  $ZrO_2/Fe_3O_4$  nanocomposites showed the presence of 100 % of the respective elements showing the purity of the as synthesized nanomaterials.

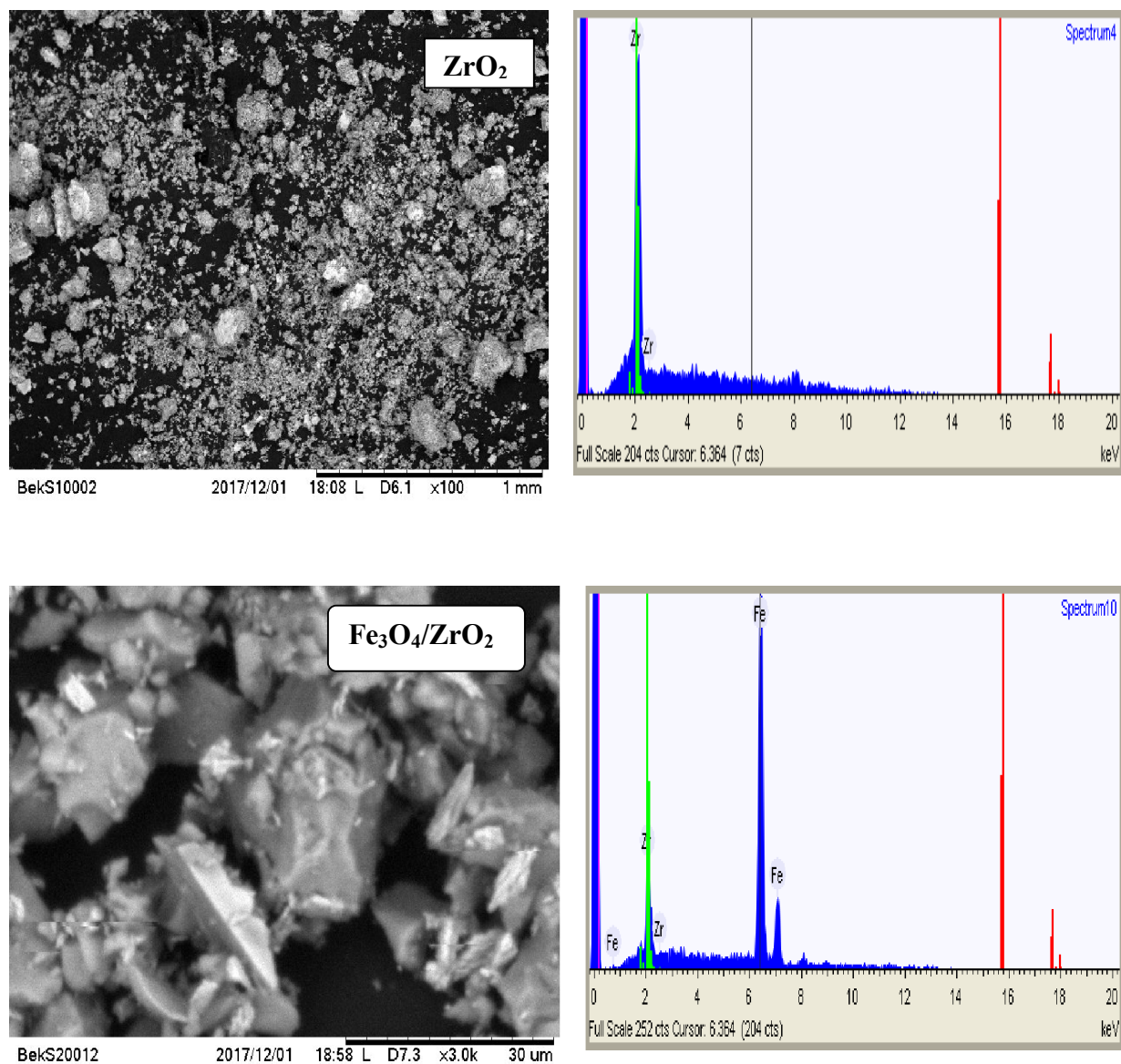


Figure 9. SEM-EDX images of  $ZrO_2$  and  $Fe_3O_4/ZrO_2$  nanocomposite

#### 4.1.3. FTIR Analysis

The FTIR spectra of the as synthesised nanomaterials are displayed in Figure 10. The absorption bands observed from  $(3500-3000\text{ cm}^{-1})$  and centered at  $3381$ ,  $3414$  and  $3368\text{ cm}^{-1}$  represent O-H stretching vibrations due to adsorbed water molecules. The absorption band observed at  $1617$  could be attributed to H-O-H bending vibration. The absorption peak at  $589\text{ cm}^{-1}$  was assigned to the Fe-O stretching vibrations in iron oxide and also the absorption bands at  $455\text{ cm}^{-1}$  can be attributed to Zr-O stretching vibrations in  $ZrO_2$  (Jiang *et al.*, 2013).

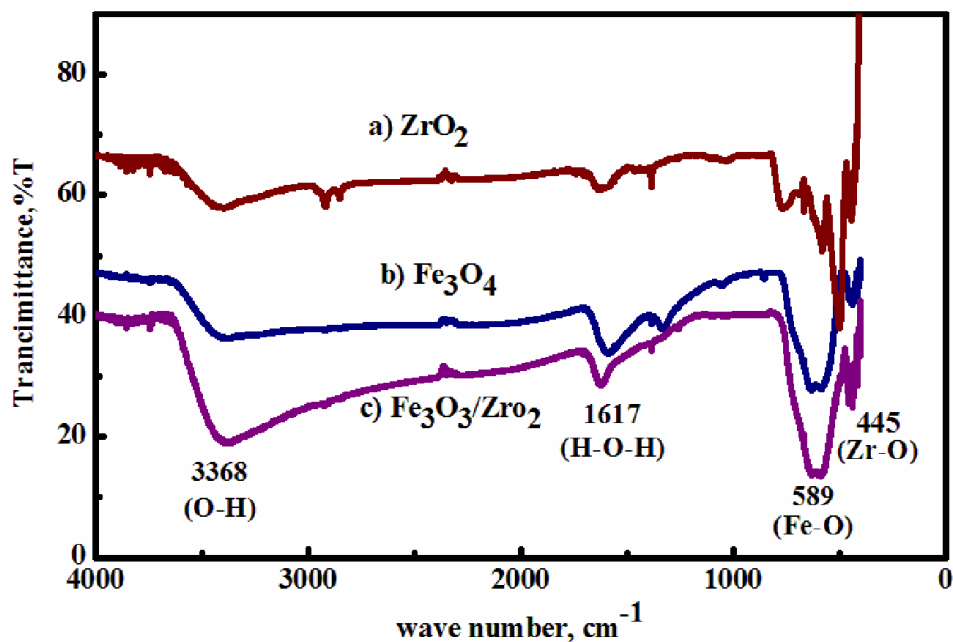


Figure 10. FTIR spectra of a) ZrO<sub>2</sub> b) Fe<sub>3</sub>O<sub>4</sub> nanoparticles and c) Fe<sub>3</sub>O<sub>4</sub>/ZrO<sub>2</sub> nanocomposite

#### 4.1.1. UV-Vis Results Analysis

Electronic absorption or UV-visible spectroscopy is one of the simplest and yet most useful optical techniques for studying optical and electronic properties of nanomaterials. The absorption, which corresponds to electron excitation from the valence band to conduction band, can be used to determine the nature and value of the optical band gap energy. UV-visible absorption spectral study may assist in understanding electronic structure of the optical band gap of the material. Absorption in the near ultraviolet region arises from electronic transitions associated within the sample.

Band gap energy of the material can be calculated using the following Eqn:

$$E_g = 1240/\lambda_g \quad (v)$$

Where,  $E_g$  is band gap energy (eV) and  $\lambda_g$  is absorption edge wavelength (nm)

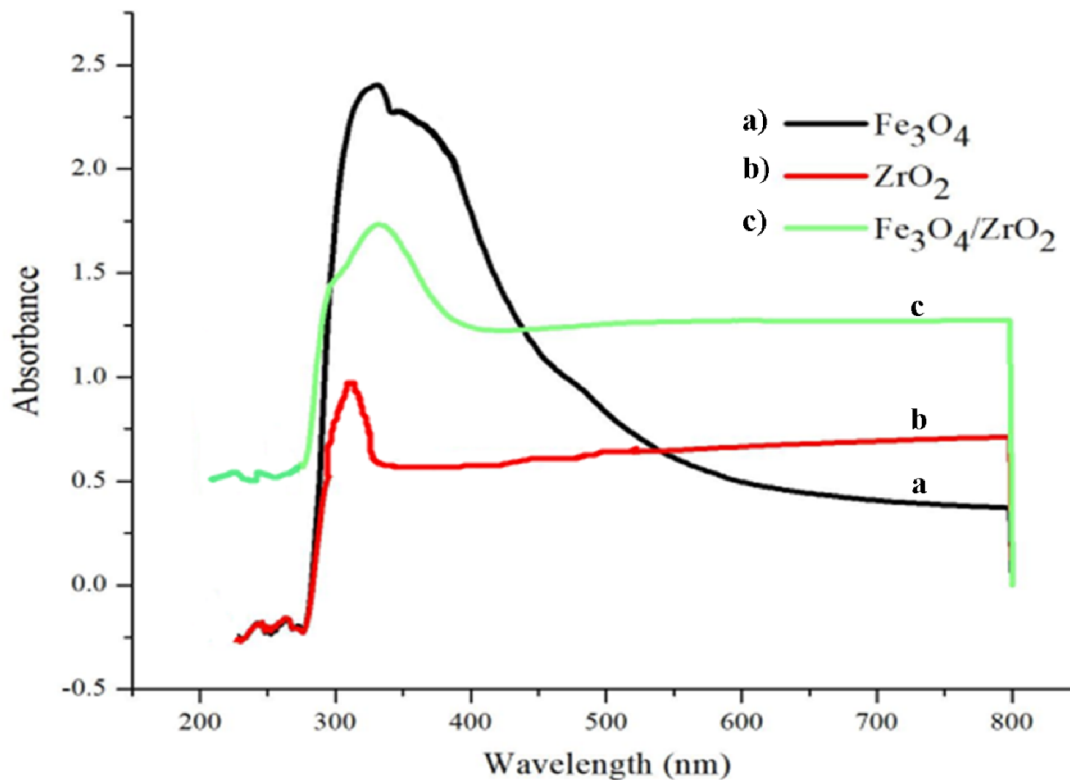


Figure 11. UV-Vis spectra of  $\text{Fe}_3\text{O}_4$ ,  $\text{ZrO}_2$  nanoparticles and  $\text{Fe}_3\text{O}_4/\text{ZrO}_2$  nanocomposite

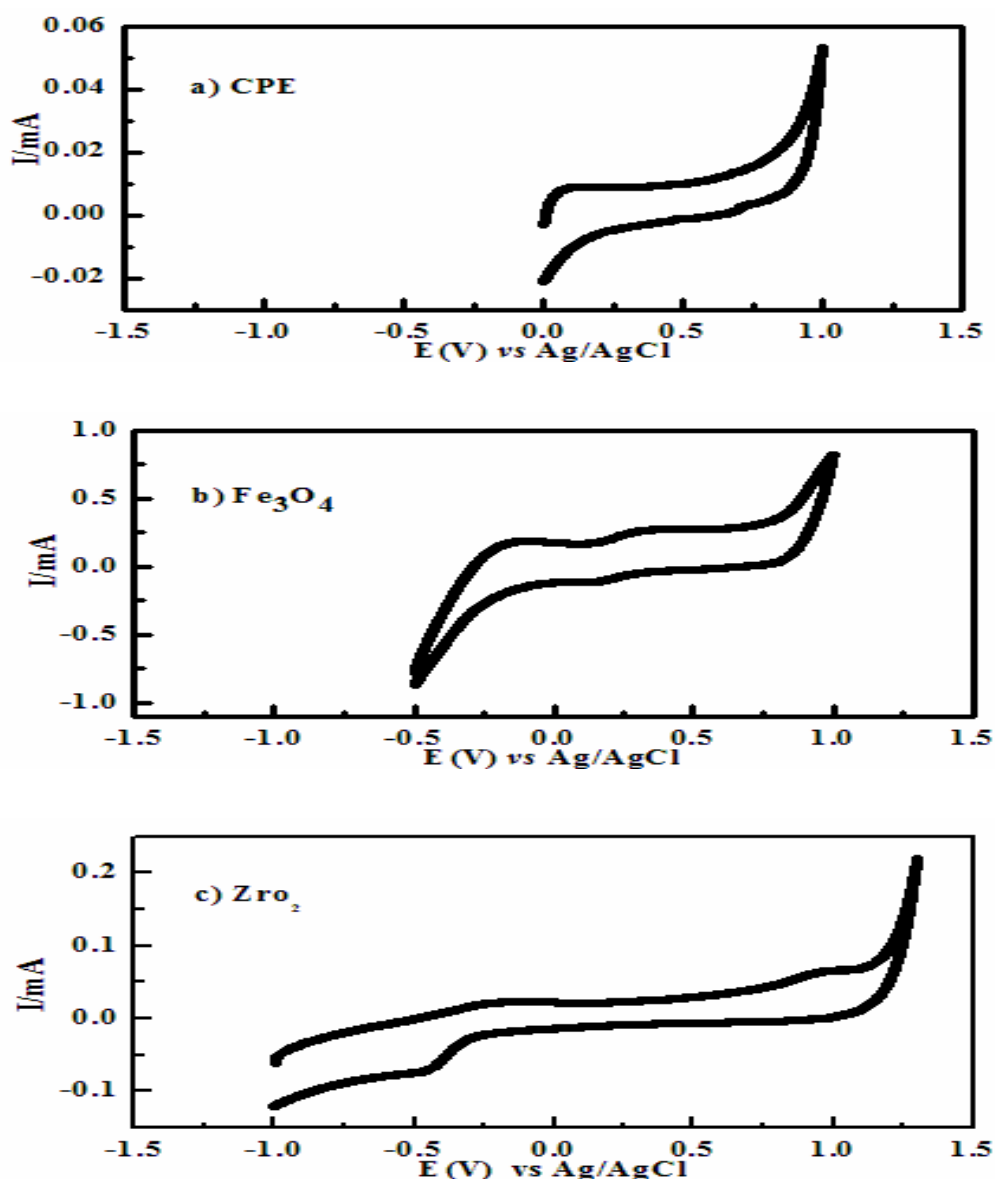
Figure 11 allows the UV-visible spectra of  $\text{Fe}_3\text{O}_4$ ,  $\text{ZrO}_2$  nanoparticles and  $\text{Fe}_3\text{O}_4/\text{ZrO}_2$  nanocomposite. For as synthesized  $\text{ZrO}_2$  nanoparticles, the strong absorption bands at low wavelength near 371 nm correspond to band gap energy of 3.5 eV approximately similar with reported in the literature. The strong absorption band of  $\text{Fe}_3\text{O}_4$  and  $\text{Fe}_3\text{O}_4/\text{ZrO}_2$  at low wavelength near 532 nm and 551 nm correspond to band gap energy of 2.33 and 2.25 eV, respectively in agreement with (Tang *et al.*, 2006). From the above UV-vis result  $\text{Fe}_3\text{O}_4/\text{ZrO}_2$  nanocomposite have low band gap energy than that of  $\text{Fe}_3\text{O}_4$  and  $\text{ZrO}_2$  nanoparticles. Therefore, the lower band gap energy provides a good electron transfer for sensor application.

## 4.2. Electrochemical Investigation

### 4.2.1. Potential Windows of Electrode Features

The potential window can be determined from a cyclic voltammogram, which is a constant region that exhibits the minimal current response (Rajawat *et al.*, 2012). The range of potential within the potential window is useful for the evaluation of electroactive species. As described in

Figure 12. CVs of CPE,  $\text{ZrO}_2/\text{CPE}$ ,  $\text{Fe}_3\text{O}_4/\text{CPE}$  and  $\text{Fe}_3\text{O}_4/\text{ZrO}_2/\text{CPE}$  electrodes in aq. KCl (0.1 M), the respective limits of potential windows were from +1.0 to 0.0 V (CPE), +1.0 to -0.5 V ( $\text{Fe}_3\text{O}_4/\text{CPE}$ ), +1.2 to -1.0 V ( $\text{ZrO}_2/\text{CPE}$ ), and +1.3 to -1.3 V ( $\text{Fe}_3\text{O}_4/\text{ZrO}_2/\text{CPE}$ ). A considerable extension of the working window with the absence of significant peak observed when  $\text{Fe}_3\text{O}_4/\text{ZrO}_2/\text{CPE}$  is used. Although the working window at the anodic and cathodic regions deteriorates, this is due to the electrocatalyzed oxidation reduction of the aqueous electrolyte or the reactivity of  $\text{Fe}_3\text{O}_4/\text{ZrO}_2/\text{CPE}$  giving rise to a limiting current appearing at about -1.3 to +1.3 V. This limiting current, however, diminishes in subsequent cycles allowing the potential working window to be widened at the anodic region to near 1.3 V as shown in Figure 12.



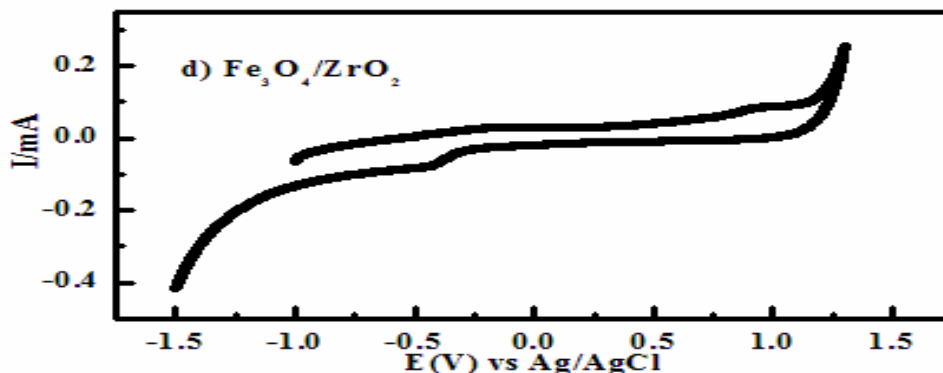


Figure 12. Potential Windows CVs of various electrodes in aq. KCl (0.1 M),  $v = 100 \text{ mVs}^{-1}$

#### 4.2.2. Cyclic Voltammetry of Potassium Ferricyanide on Various Modified CPE

Bass100B electrochemical Bioanalyzer and Ag/AgCl (3M KCl) reference electrode working status was tested using potassium ferrocyanide (2 mM  $\text{K}_3\text{Fe}(\text{CN})_6$ ) solution in 0.1 M KCl a well-known model compound for reversible process.  $\text{K}_3\text{Fe}(\text{CN})_6$  was also used as a redox probe by studying its voltammetric behavior both on bare and modified CP electrode. Cyclic voltammogram of 2 mM  $\text{K}_3\text{Fe}(\text{CN})_6$  in a potential range from  $-0.2$  and  $0.6$  V is shown in (Figure 13) and its various electrochemical parameters are evaluated and summarized in Tables 2, 3, 4 and 5.

The electrochemical cycling behavior of the CPE,  $\text{Fe}_3\text{O}_4/\text{CPE}$ ,  $\text{ZrO}_2/\text{CPE}$  and  $\text{Fe}_3\text{O}_4/\text{ZrO}_2/\text{CPE}$  were studied using cyclic voltammograms as shown in Figure 13. The effects of scan rate on peak potential were examined at different scan rates from  $10$  to  $100 \text{ mVs}^{-1}$ . Linear relationships were observed between the scan rates and peak current of the electrode. Therefore, an increase in scan rate results to an increase in the peak potential. Both the anodic and cathodic peak potentials show a slight shift towards the positive potential. Hence, the peak-to-peak separation decreases with an increase in scan rate and ratio of peak currents were nearly 1, showing the reversibility of the process (Roa *et al.*, 2003, Beltagi *et al.*, 2011).

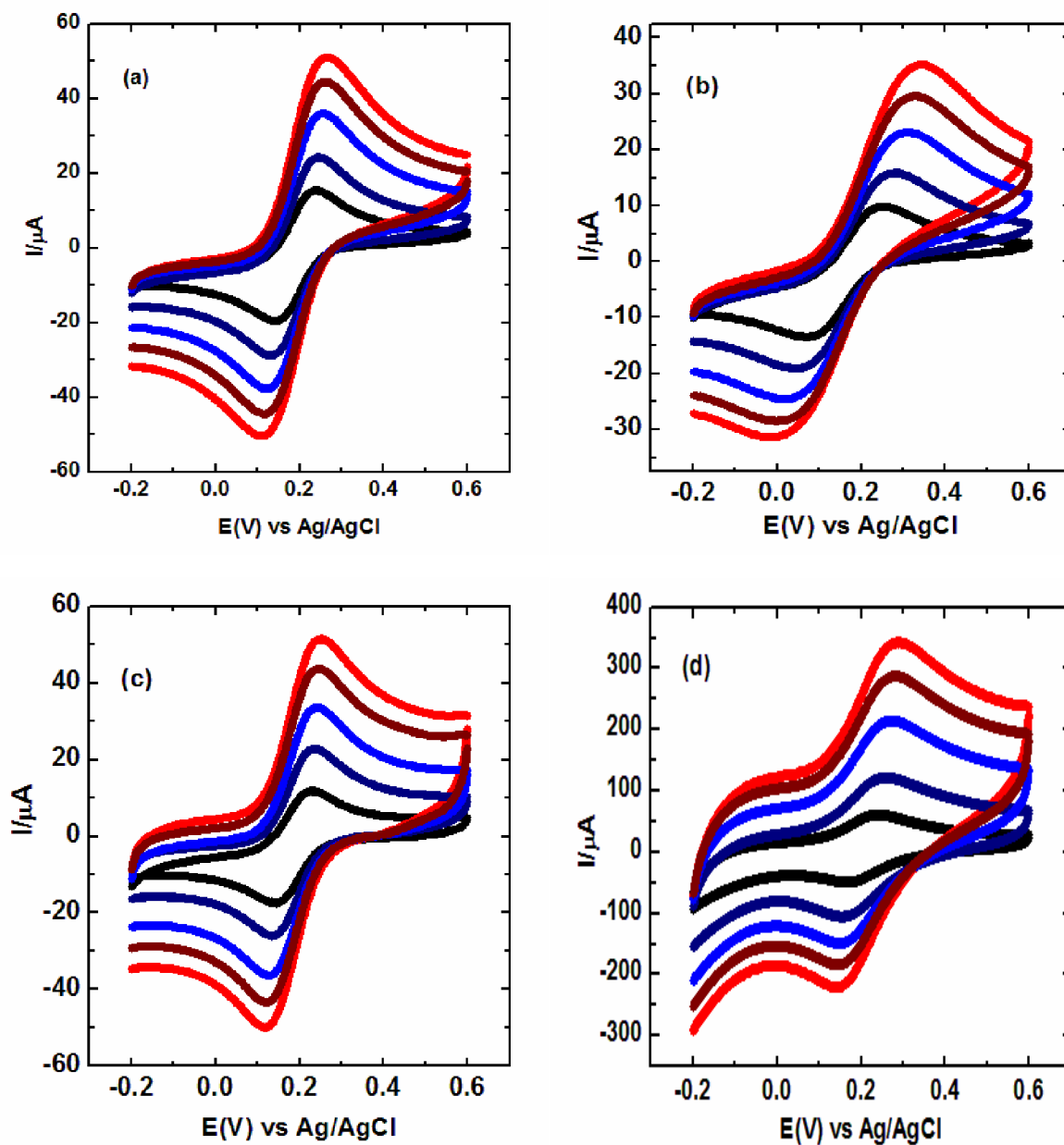


Figure 13. CVs of a) CPE, b)  $\text{Fe}_3\text{O}_4/\text{CPE}$ , c)  $\text{ZrO}_2/\text{CPE}$  and d)  $\text{Fe}_3\text{O}_4/\text{ZrO}_2/\text{CPE}$  (at 10, 25, 50, 75 and  $100 \text{ mV s}^{-1}$  scan rates) in 2 mM of  $\text{K}_3\text{Fe}(\text{CN})_6$  in 0.1 M KCl

The Ag/AgCl reference electrode was calibrated using  $\text{K}_3\text{Fe}(\text{CN})_6$ . The redox potential of  $\text{K}_3\text{Fe}(\text{CN})_6^{-4/3-}$  was found to be 0.187 V. This result was lower by 0.0865 V from the literature value of 0.2735 V. Therefore, 0.0865 V is added to all electrochemical measurements and all potentials reported calibrated reference to Ag/AgCl electrode.

The electroactive surface areas of the pure CPE, Fe<sub>3</sub>O<sub>4</sub>/CPE, ZrO<sub>2</sub>/CPE and Fe<sub>3</sub>O<sub>4</sub>/ZrO<sub>2</sub>/CPE were also estimated by performing CV in the range of 0.2 to 0.6 V for 2 mM K<sub>3</sub>Fe(CN)<sub>6</sub><sup>-4/3-</sup> in 0.1 M KCl. The slope of  $I_{pa}$  vs.  $v^{1/2}$  curve was obtained by varying scan rate from 0.01 to 0.1 V/s and the electroactive surface area was calculated from the Randles-Sevcik equation for a reversible process.

$$I_{pa} = 2.687 \times 10^5 n^{3/2} A D^{1/2} V^{1/2} C \quad (vi)$$

Where n is the number of electrons participating in the redox reaction, A is the area of the electrode (cm<sup>2</sup>), D is the diffusion coefficient (cm<sup>2</sup>s<sup>-1</sup>), C is the concentration of K<sub>3</sub>Fe(CN)<sub>6</sub> in M. (molcm<sup>-3</sup>), and V is the scan rate (V s<sup>-1</sup>). For 2.0×10<sup>-3</sup> K<sub>3</sub>Fe(CN)<sub>6</sub> in 0.1 M KCl electrolyte, n = 1 and D = 5.15×10<sup>-6</sup> cm<sup>2</sup> s<sup>-1</sup>, then from the slope of the  $I_{pa}$  vs.  $V^{1/2}$ , the surface area of the electrode can be calculated. The average values of the electroactive surface area were 0.0458, 0.046, 0.069 and 0.0978 cm<sup>2</sup> for CPE, Fe<sub>3</sub>O<sub>4</sub>/CPE, ZrO<sub>2</sub>/CPE and Fe<sub>3</sub>O<sub>4</sub>/ZrO<sub>2</sub>/CPE respectively. These results indicate that Fe<sub>3</sub>O<sub>4</sub>/ZrO<sub>2</sub>/CPE has higher electroactive surface area than CPE.

Table 2. The effect of scan rate on peak current using CPE in 2 mM K<sub>3</sub>Fe (CN)<sub>6</sub>

Scan rate(mV/s)	$i_{pa}$ ( $\mu$ A)	$E_{pa}$ (mV)	$i_{pc}$ ( $\mu$ A)	$E_{pc}$ (mV)	$i_{pa}/i_{pc}$ ( $\mu$ A)	$\Delta E_p$ (mV)
10	15	240	-19	141	0.8	99
25	25	246	-28	128	0.9	118
50	37	258	-37	115	1	143
75	44	265	-44	110	1	155
100	51	271	-50	103	1.02	168

Table 3. The effect of scan rate on peak current using Fe<sub>3</sub>O<sub>4</sub>/CPE in 2 mM K<sub>3</sub>Fe (CN)<sub>6</sub>

Scan rate(mV/s)	<i>i</i> <sub>pa</sub> (μA)	<i>E</i> <sub>pa</sub> (mV)	<i>i</i> <sub>pc</sub> (μA)	<i>E</i> <sub>pc</sub> (mV)	<i>i</i> <sub>pa</sub> / <i>i</i> <sub>pc</sub> (μA)	$\Delta E_p$ (mV)
10	10.3	235	-13.5	128	0.76	107
25	16	264	-18.7	114	0.86	150
50	23.5	286	-24.4	107	0.94	179
75	29.8	300	-28	92	1.1	208
100	35	329	-31	85	1.13	244

Table 4. The effect of scan rate on peak current using ZrO<sub>2</sub>/CPE in 2 mM K<sub>3</sub>Fe (CN)<sub>6</sub>

Scan rate(mV/s)	<i>i</i> <sub>pa</sub> (μA)	<i>E</i> <sub>pa</sub> (mV)	<i>i</i> <sub>pc</sub> (μA)	<i>E</i> <sub>pc</sub> (mV)	<i>i</i> <sub>pa</sub> / <i>i</i> <sub>pc</sub> (μA)	$\Delta E_p$ (mV)
10	12	226	-17	141	0.7	85
25	23	239	-24	134	0.96	105
50	33	240	-35	128	0.94	112
75	44	248	-42	118	1.05	130
100	51	253	-49	117	1.05	136

Table 5. The effect of scan rate on peak current using Fe<sub>3</sub>O<sub>4</sub>/ZrO<sub>2</sub>/CPE in 2 mM K<sub>3</sub>Fe (CN)<sub>6</sub>

Scan rate(mV/s)	<i>i</i> <sub>pa</sub> (μA)	<i>E</i> <sub>pa</sub> (mV)	<i>i</i> <sub>pc</sub> (μA)	<i>E</i> <sub>pc</sub> (mV)	<i>i</i> <sub>pa</sub> / <i>i</i> <sub>pc</sub> (μA)	$\Delta E_p$ (mV)
10	63	242	-47	161	1.3	81
25	127	257	-104	145	1.2	112
50	216	261	-146	138	1.5	123
75	289	289	-179	144	1.6	124
100	344	344	-220	145	1.6	129

### 4.2.3. Electrochemical Impedance Spectroscopy

The bare CPE,  $\text{Fe}_3\text{O}_4/\text{CPE}$ ,  $\text{ZrO}_2/\text{CPE}$  and  $\text{Fe}_3\text{O}_4/\text{ZrO}_2/\text{CPE}$  was also characterized by EIS using  $\text{K}_3\text{Fe}(\text{CN})_6^{-4/3-}$  as electrochemical redox probes. In electrochemical impedance measurement, the semicircle diameter of impedance equals the electron transfer resistance ( $R_{et}$ ), which controls the electron transfer kinetics of the redox probe at the electrode surface. Figure 14 presented the Nyquist diagrams of the bare CPE (curve a) and  $\text{Fe}_3\text{O}_4/\text{CPE}$  (curve b),  $\text{ZrO}_2/\text{CPE}$  (curve c) and  $\text{Fe}_3\text{O}_4/\text{ZrO}_2/\text{CPE}$  (curve d) in 0.1 M KCl containing 2.0 mM  $\text{K}_3\text{Fe}(\text{CN})_6^{-4/3-}$ . As it has been seen, the semi-circle of the high frequency region of the  $\text{Fe}_3\text{O}_4/\text{ZrO}_2$  modified CPE electrode was smaller than that of the bare CPE. This can be attributed to the incorporation of the  $\text{Fe}_3\text{O}_4$  and  $\text{ZrO}_2$  nanoparticles with good conductivity and large surface area into carbon paste, which could effectively increase the electron transfer rate between electrode surface and probe and decrease interface electron transfer resistance. The calculated charge transfer resistance values for the CPE,  $\text{Fe}_3\text{O}_4/\text{CPE}$ ,  $\text{ZrO}_2/\text{CPE}$  and  $\text{Fe}_3\text{O}_4/\text{ZrO}_2/\text{CPE}$  were 3108, 2420, 2168 and 976  $\Omega$  respectively.

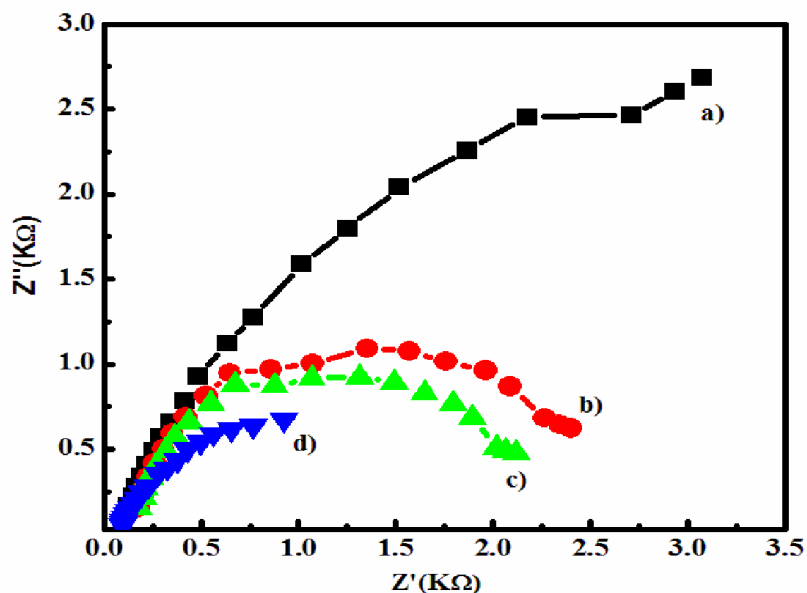


Figure 14. Electrochemical impedance spectroscopy of a) CPE, b)  $\text{Fe}_3\text{O}_4/\text{CPE}$ , c)  $\text{ZrO}_2/\text{CPE}$  and d)  $\text{Fe}_3\text{O}_4/\text{ZrO}_2/\text{CPE}$  in 2 mM  $\text{K}_3\text{Fe}(\text{CN})_6$  in 0.1 M KCl

### 4.3. Electrochemical Behavior of Ascorbic Acid at the Surface of Various Electrodes

The electrochemical responses of 2.5 mM AA in 0.2 M acetate buffer solution of pH 4 at the bare carbon paste electrode (BCPE) and modified carbon paste electrode prepared with the Fe<sub>3</sub>O<sub>4</sub>, ZrO<sub>2</sub> nanoparticles and Fe<sub>3</sub>O<sub>4</sub>/ZrO<sub>2</sub> nanocomposites (MCPE) with the scan rate 100 mV s<sup>-1</sup> were displayed in (Figure 15). The oxidation peak potentials of CPE, Fe<sub>3</sub>O<sub>4</sub>/CPE, ZrO<sub>2</sub>/CPE and Fe<sub>3</sub>O<sub>4</sub>/ZrO<sub>2</sub>/CPE were 0.40, 0.32, 0.24 and 0.2 V and also their oxidation peak current were 67, 167, 283 and 335 μA respectively. The results showed that the oxidation of ascorbic acid occurred at the surface of the bare CPE, but MCPE enhances the peak current and decreases the oxidation peak potential. A substantial negative shift of the currents starting from oxidation potential for AA and dramatic increase of the current indicates the electrochemical ability of Fe<sub>3</sub>O<sub>4</sub>/CPE (curve b), ZrO<sub>2</sub>/CPE (curve c) and Fe<sub>3</sub>O<sub>4</sub>/ZrO<sub>2</sub>/CPE (curve d) to AA oxidation. However, Fe<sub>3</sub>O<sub>4</sub>/ZrO<sub>2</sub>/CPE shows much higher (five folds) anodic peak current for the oxidation of AA compared to Fe<sub>3</sub>O<sub>4</sub>/CPE and ZrO<sub>2</sub>/CPE. So, indicating that the synergetic effect of Fe<sub>3</sub>O<sub>4</sub> characteristic surface adsorption process (Gholivand *et al.*, 2015) and ZrO<sub>2</sub> electro-catalytic nature (Lavanya *et al.*, 2014) had significantly improved the performance of the electrode toward AA oxidation.

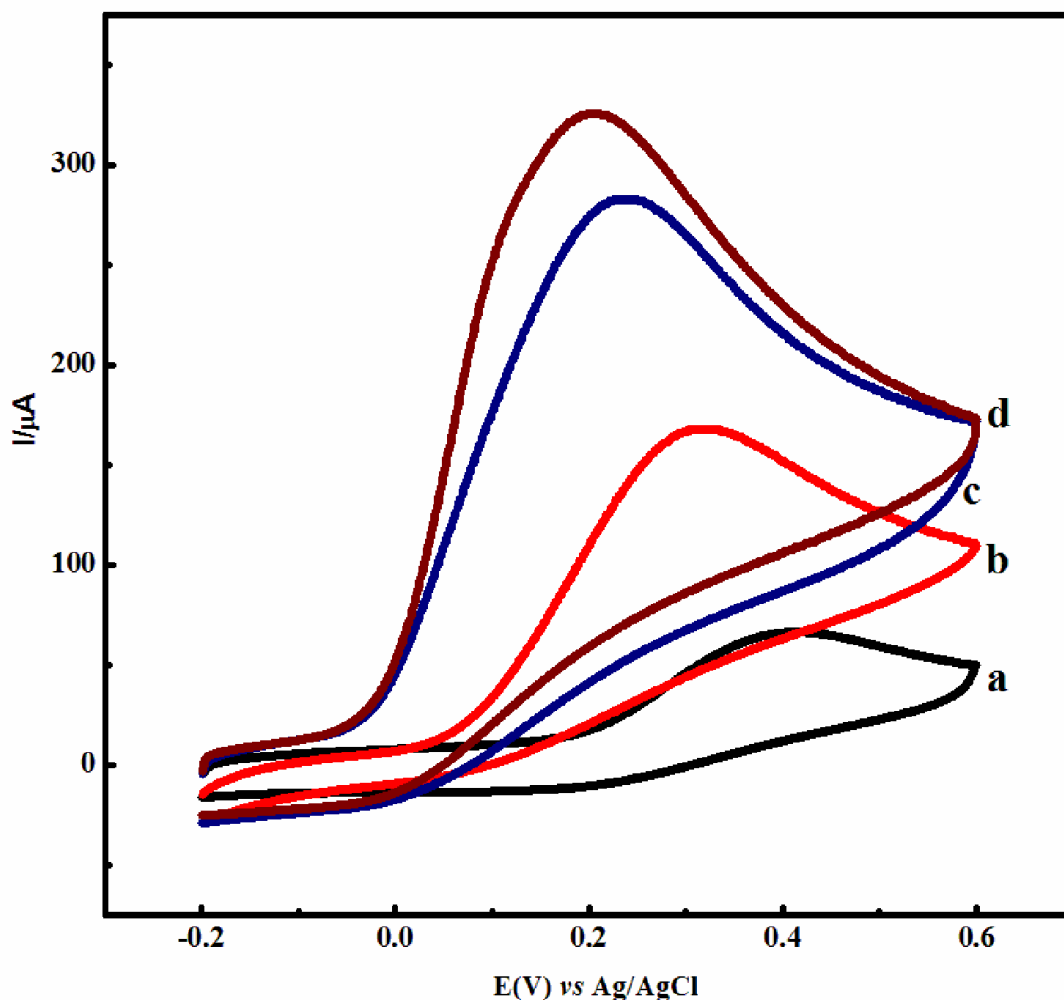


Figure 15. CVs of 2.5 mM AA a) CPE, b)  $\text{Fe}_3\text{O}_4/\text{CPE}$ , c)  $\text{ZrO}_2/\text{CPE}$  and d)  $\text{Fe}_3\text{O}_4/\text{ZrO}_2/\text{CPE}$  (pH 4,  $v=100 \text{ mV s}^{-1}$ )

#### 4.4. The Electrochemical Response of AA at $\text{Fe}_3\text{O}_4/\text{ZrO}_2/\text{CPE}$

The redox activity of as-prepared  $\text{Fe}_3\text{O}_4/\text{ZrO}_2/\text{CPE}$  materials was investigated using cyclic voltammetry in 0.1 M ABS. Figure 16. shows cyclic voltammograms for absence and presence of AA in the potential range from -0.5 to +1.3 V, at a scan rate of  $100 \text{ mVs}^{-1}$ . There is no redox activity observed in the absence of AA. However, the presence of AA showed only an oxidation peak without its reduction pair. The result shows that, the AA shows an irreversible electrochemistry, characterized by the presence of the oxidation peak without its reduction pair.

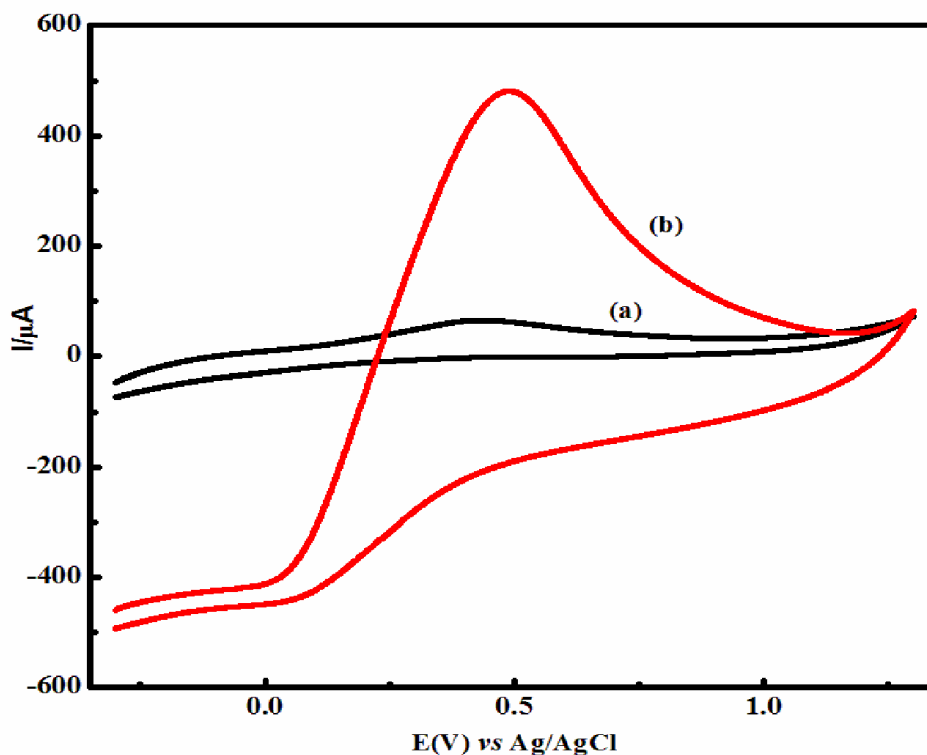


Figure 16. Cyclic voltammograms of 0.2 M acetate buffer (pH 4) in the absence (a) and presence (b) of 2.5 mM AA at the  $\text{Fe}_3\text{O}_4/\text{ZrO}_2/\text{CPE}$

## 4.5. Optimization of Experimental Parameters for Ascorbic Acid Detection

### 4.5.1. Effect of Scan Rate

The effect of a varying scan rate on the oxidation process of ascorbic acid was studied. Cyclic voltammograms of 2.5 mM ascorbic acid in 0.1 M ABS supporting electrode using a  $\text{Fe}_3\text{O}_4/\text{ZrO}_2/\text{CPE}$  modified electrode was obtained for the scan rate from 10 to 100  $\text{mV s}^{-1}$  Figure 17a. Good linearity between the anodic peak current and square root of scan rate was obtained by  $y = 104.45x + 106.15$  with  $R^2 = 0.9976$  Figure 17b, which supports the idea that the electrode reactions of ascorbic acid were under diffusion control. Figure 17c shows the plot of  $\log I_{pa}$  (peak current) of versus  $\log v$  (scan rate). A linear relationship between the peak current and the scan rate is described by  $y = 0.46409x + 2.13624$ , where  $R^2 = 0.99895$ . The oxidative current of ascorbic acid increased with the scan rate is due to heterogeneous kinetics. The slope of 0.46 is comparable with the theoretical slope of 0.5 for a diffusion controlled process (Zidan, *et al.*, 2011).

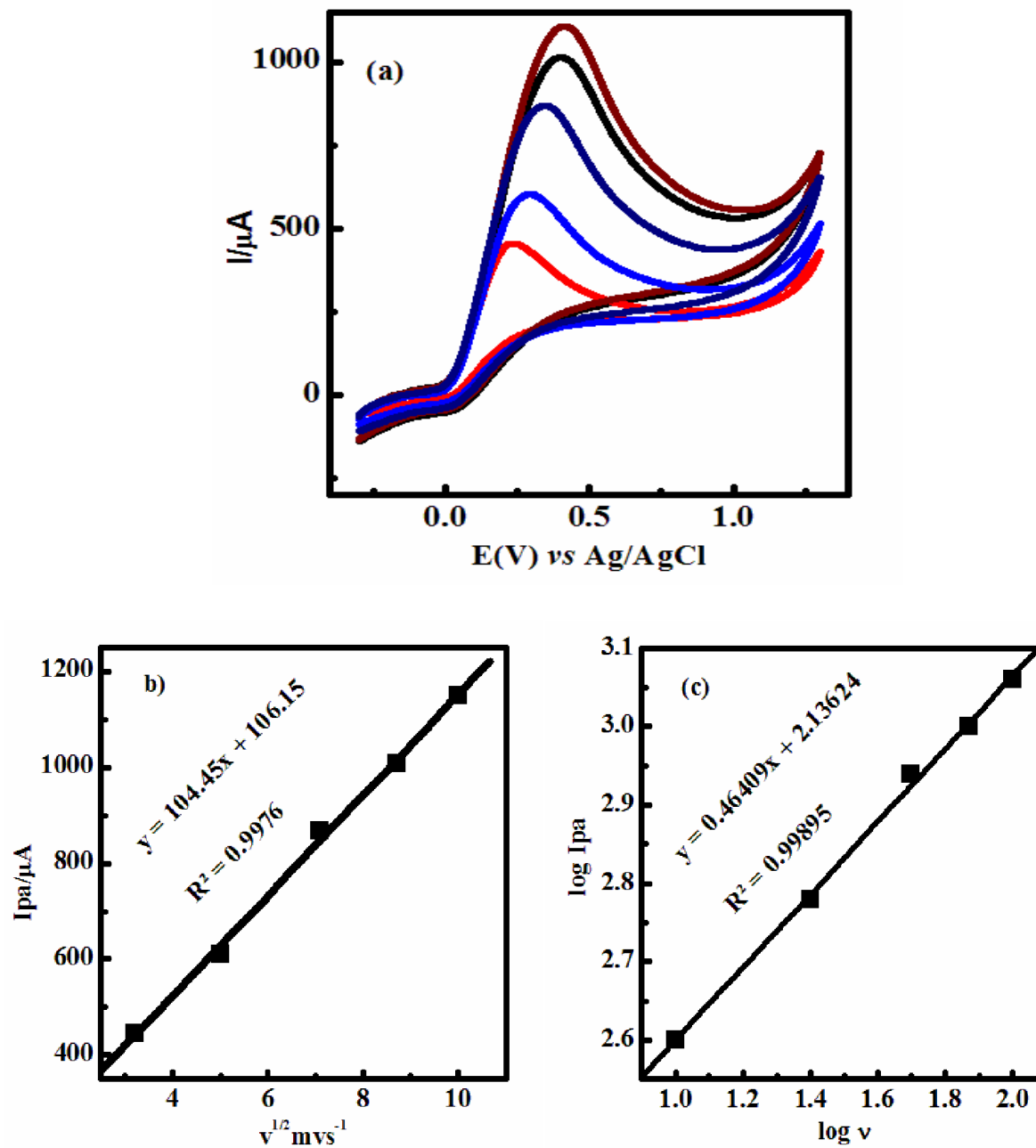
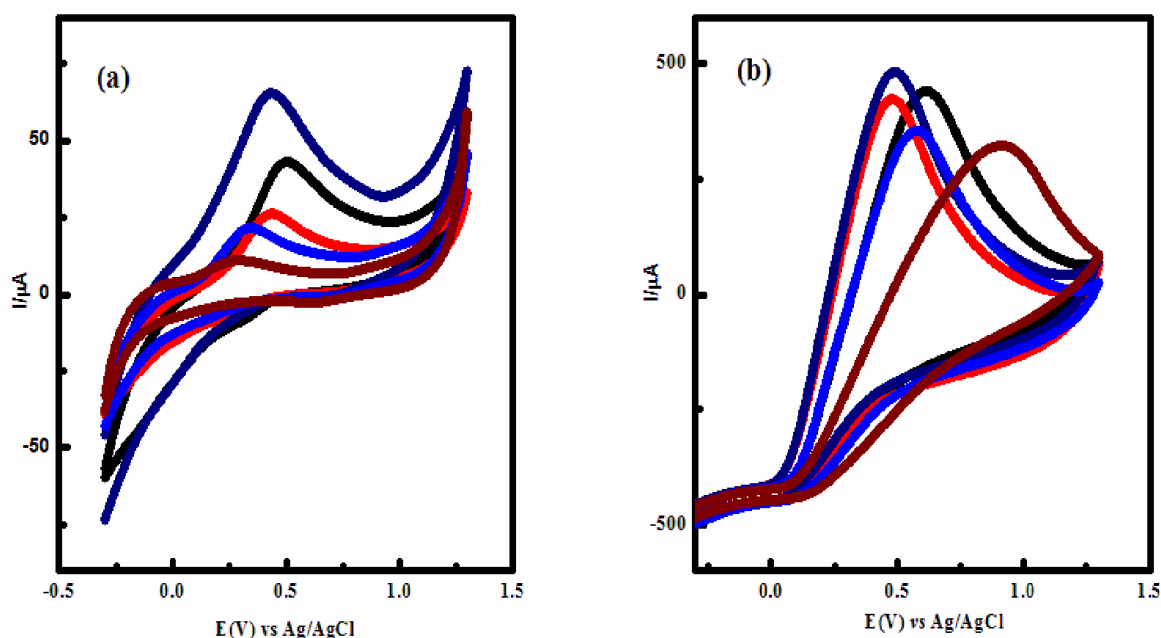


Figure 17. (a) CVs of  $\text{Fe}_3\text{O}_4/\text{ZrO}_2/\text{CPE}$  in 0.1 M ABS (pH 4) containing 2.5 mM AA at various scan rates; 10, 25, 50, 75 and 100  $\text{mV s}^{-1}$  (b) The plot of anodic peak current vs. square root of the scan rate (c) The plot of log peak current vs. log the scan rate.

#### 4.5.2. Effect of pH

Cyclic voltammetry was used to investigate the effects of pH value in the determination of AA at Fe<sub>3</sub>O<sub>4</sub>/ZrO<sub>2</sub> modified CPE. Figure 18 a and b shows cyclic voltammograms obtained at Fe<sub>3</sub>O<sub>4</sub>/ZrO<sub>2</sub> modified CPE in 0.2 M Acetate buffer solutions of different pH values with and without 2.5 mM AA at scan rates of 100 mV s<sup>-1</sup>. As illustrated in Figure 18c the anodic peak current was increased with pH, and reached its maximum value at pH 4. Further increase in the pH value decreases the response of the electrode. Thus, pH 4.0 was taken as the optimum pH value for subsequent investigations.

Furthermore, the effect of solution pH on the peak potential for AA at Fe<sub>3</sub>O<sub>4</sub>/ZrO<sub>2</sub>/CPE was studied. The potential shifted negatively with increasing pH, suggesting the involvement of protons in electrochemical process of AA Figure 18d. The relationship between the peak potential and the pH can be described as:  $E_{pa} \text{ (V)} = -0.065\text{pH} + 0.702$ ,  $R^2 = 0.9977$ . The slope 0.065 V/pH is close to the theoretical value 0.059 V/pH (at 25 °C) given by the Nernstian equation, which indicates equal numbers of protons and electrons participate in the oxidation of AA as described in Figure 2.



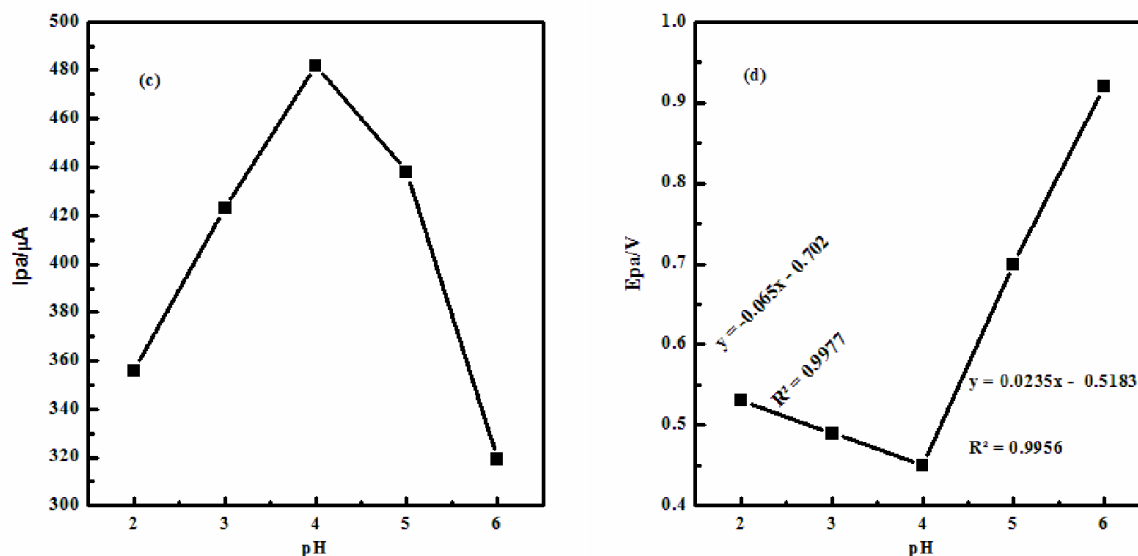


Figure 18. CVs obtained at  $Fe_3O_4/ZrO_2/CPE$  in 0.2 M ABS in pH values (2, 3, 4, 5 and 6) containing 2.5 mM AA at scan rate  $100 \text{ mV s}^{-1}$ ; c) Variations in the oxidation peak current as a function of pH d) Variations in the oxidation peak potential as a function of pH.

#### 4.6. Application of $Fe_3O_4/ZrO_2/CPE$ Electrode for the Determination of AA

The differential pulse voltammetric technique was used for the analysis of AA concentration in standard solutions from 1 to 6  $\mu M$  shown under optimized experimental condition (pH = 4 and  $100 \text{ mV s}^{-1}$  scan rate). The response of  $Fe_3O_4/ZrO_2/CPE$  sensor to the various concentration of AA is displayed in (Figure 20 a) and the plot of peak current *versus* concentration (Figure 20 b) depicts that the peak current increased linearly with increasing the AA concentration in the range from  $1.0 \times 10^{-6}$  to  $6.0 \times 10^{-6}$  M. The sensor showed high sensitivity  $11 \mu A/\mu M$ , good linear range (1 to  $6 \times 10^{-6}$  M) and a lower limit of detections (LOD) were found to be  $0.51 \mu M$  of AA by use of the formula  $LOD = 3\alpha/a$  (where ' $\alpha$ ' is the standard deviation of residuals and 'a' is the slope of the calibration plot).

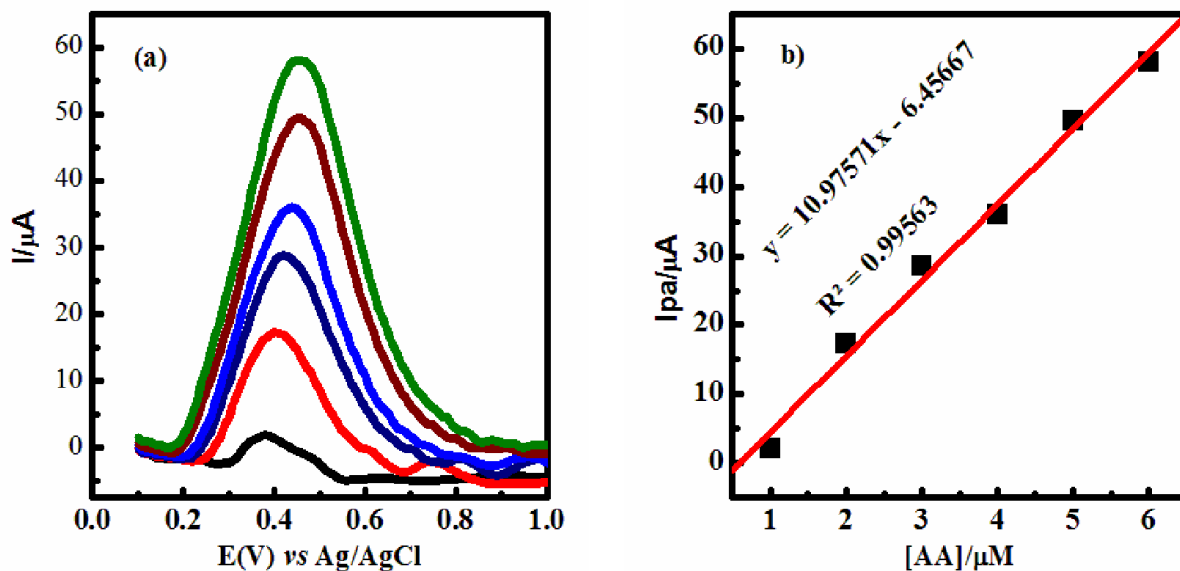


Figure 19. (a) DPVs of AA on Fe<sub>3</sub>O<sub>4</sub>/ZrO<sub>2</sub>/CPE in 0.2 M ABS (pH 4) (b) variations of peak current as a function of AA concentration

Table 6. Comparison of the present work with previous reported ones

Modified electrodes	Method	Linear range(μM)	Detection limit (μM)	Reference
Polyaniline MGCE and screen printed electrodes	DPV	1-100	2.45	O'Connell <i>et al.</i> , 2001
MnO <sub>2</sub> graphite composite electrode	CV	0-2.5 mol L <sup>-1</sup>	0.4	Langley <i>et al.</i> , 2007
Carbon fiber microelectrode/nickel oxide and ruthenium hexacyanoferrate	Amperometric	10-1610	1	Hutton <i>et al.</i> , 2010
Graphene doped/CPE	Amperometric	10 – 106	0.17	Li <i>et al.</i> , 2011
MWCNT/CPE	SWV	0.02-140	0.091	Keyvanfard <i>et al.</i> , 2013
Fe <sub>3</sub> O <sub>4</sub> /ZrO <sub>2</sub> /CPE	DPV	1-6	0.51	Present work

#### 4.7. Detection of Ascorbic Acid in paracetamol

The systematic measurement first for the solution containing only the supporting electrolyte and then aliquot of the standard solutions were added for the AA analysis in the standard solution using DPV. Paracetamol sample did not contain detectable amount of AA, hence the sample was spiked with  $1.0 \times 10^{-6}$  M AA standard solution. From the calibration curves plotted for the known standard solution of AA, the unknown concentration of AA (value of X) was successfully calculated by using equation  $y = A + B \cdot X$  obtained from the calibration curves of the standard solution. In this case the value of “A” is intercept and B (slope) and the value of y (peak current) was obtained from the DPV Figure 19 recorded for AA in paracetamol sample. In such extracted sample, satisfactory recovery (94.4 %) of the experimental results was found for AA. These values show that the method was valid for the determination of pharmaceutical sample under study.

#### 4.8. Reproducibility and Stability

When the concentration of ascorbic acid was controlled at 2  $\mu$ M, good reproducibility was observed with relative standard deviation (R.S.D.) of 2.4 % for five consecutive detections as shown in (Appendix Table 1). This level of precision is suitable for the routine quality control analysis of the drug in pharmaceutical dosage form and biological fluids. The sensor retained a response of 96.91 % of the initial current after 30 days storage of the electrode at room temperature (Appendix Table 2) and no obvious decline was observed after using the electrode 5 times. The  $\text{Fe}_3\text{O}_4/\text{ZrO}_2/\text{CPE}$  after n number of days 96.77 %  $\pm$  0.147 % stability was observed as shown in Figure 20.

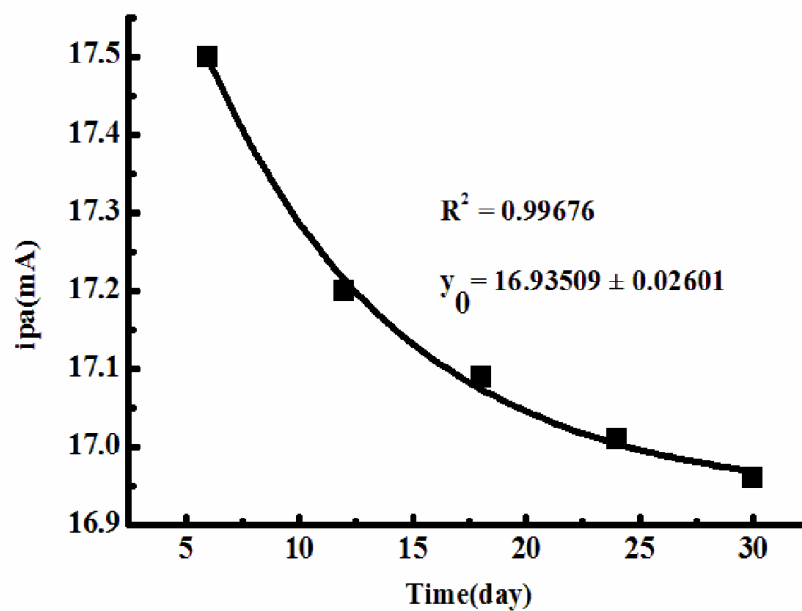


Figure 20.  $\text{Fe}_3\text{O}_4/\text{ZrO}_2/\text{CPE}$  Variation peak current with time in  $2 \mu\text{A}$  AA in  $0.2 \text{ M}$  ABS (pH 4)

## 5. SUMMARY, CONCLUSION AND RECOMMENDATION

### 5.1. Summary and Conclusion

$\text{Fe}_3\text{O}_4$ ,  $\text{ZrO}_2$  and  $\text{Fe}_3\text{O}_4/\text{ZrO}_2$  nanocomposite were successfully synthesized by co-precipitation method. The structural and morphological properties of the materials were characterized by FTIR, UV-Vis, XRD and SEM. The FTIR spectra confirmed the presence of function groups in all prepared nanomaterials. Moreover, uv-vis spectra of  $\text{Fe}_3\text{O}_4/\text{ZrO}_2$  showed the presence of magnetite and zirconium oxide components. The band gap energy of  $\text{ZrO}_2$  was 3.34 eV and  $\text{Fe}_3\text{O}_4$  2.33 eV slightly greater than that of the nanocomposite (2.25 eV). XRD patterns  $\text{Fe}_3\text{O}_4/\text{ZrO}_2$  nanocomposite reveals particle size of 9.8 nm a small in comparison to the single systems indicating its potential for sensor application.

Electrochemical properties of carbon paste electrode and modified one by  $\text{Fe}_3\text{O}_4$ ,  $\text{ZrO}_2$  and  $\text{Fe}_3\text{O}_4/\text{ZrO}_2$  nanocomposite were investigated in the presence of 2 mM potassium ferrocyanide in 0.1 M KCl employing cyclic voltammetry.  $\text{ZrO}_2/\text{Fe}_3\text{O}_4/\text{CPE}$  revealed enhanced peak current and small peak to peak separation. The fact that magnetite has a high absorption capacity together with  $\text{ZrO}_2$  high surface area and good catalytic property, improves the electrical signal of the nanocomposite. Besides, on all electrodes the electrode probe behaves a reversible process, particularly the CPE modified by the binary system showed small peak to peak separation potential. Furthermore, the high conductivity of  $\text{ZrO}_2/\text{Fe}_3\text{O}_4/\text{CPE}$  was supported by EIS spectra which results low charge transfer resistance.

Since  $\text{Fe}_3\text{O}_4/\text{ZrO}_2$  nanocomposites performed very well in the presence of potassium ferrocyanide,  $\text{Fe}_3\text{O}_4/\text{ZrO}_2/\text{CPE}$  sensor pH and scan rate experimental parameters were optimized for the detection of ascorbic acid in acetate buffer solution. Using the optimized condition (pH = 4 and scan rate of  $100 \text{ mV s}^{-1}$ ) the electrode was used to determine ascorbic acid in standard solution from  $1$  to  $6 \times 10^{-6} \text{ M}$  AA by applying DPV. The sensor showed detection limit of  $6 \times 10^{-7} \text{ M}$ , good electrochemical sensitivity towards the AA  $11 \mu\text{A}/\mu\text{M}$  and linear range of  $1$  to  $6 \times 10^{-6} \text{ M}$ . Besides, the electrode was 2.4 % reproducibility and 96.91 % stability. The result indicated that the electrode has a similar performance to CPE modified by other materials in the literature.  $\text{Fe}_3\text{O}_4/\text{ZrO}_2/\text{CPE}$  sensor was also used to determine AA in paracetamol. The concentration of AA was not detected in paracetamol sample. So its content in the drug was determined by spiking  $1 \times$

$10^{-6}$  M the concentration of AA in paracetamol was estimated to be  $0.944 \times 10^{-6}$  M. Therefore, the developed sensor can be used for the analysis of AA in various samples.

## 5.2. Recommendation

Taking in to account the limitations observed in this study the following are recommended for future research.

- ✚ To understand the best performance of  $\text{Fe}_3\text{O}_4/\text{ZrO}_2$  modified carbon paste electrode studying at various ratio and composition of  $\text{Fe}_3\text{O}_4$ ,  $\text{ZrO}_2$ , graphite and paraffin oil is recommended for future investigations.
- ✚ Detail electrochemical characterization  $\text{Fe}_3\text{O}_4/\text{ZrO}_2/\text{CPE}$ , optimization of experimental parameters such as absorption time and characteristic parameterizes of differential pulse voltammetry is critical to understand the behaviors of the electrode.
- ✚ In this study  $\text{Fe}_3\text{O}_4/\text{ZrO}_2$  was used as carbon paste electrode modifier, other metal oxides and nanocomposites can be used to modify CPE and studied for the detection of ascorbic acid in various samples.

## 6. REFERENCES

- Abu-Shawish, H.M., Saadeh, S.M., Dalloul, H.M., Najri, B., Al Athamna, H. 2013. Modified carbon paste electrode for potentiometric determination of silver (I) ions in burning cream and radiological films. *Sensors and Actuators B*, 182: 374-381.
- Adams, N.R. 1976. Probing brain chemistry with electro analytical technique. *Analytical chemistry*, 48(14): 1126-1138.
- Aglan, R.F., Mohamed, G.G., Mohamed, H.A. 2012. Chemically modified carbon paste electrode for determination of cesium ion by potentiometric method. *American Journal of Analytical Chemistry*, 3: 576–586.
- Agraz, R., Sevilla, M.T., Pinilla, J.M., Hernandez, L. 1991. Voltammetric determination of cadmium on a carbon paste electrode modified with a chelating resin. *Electroanalysis*, 3: 393-397.
- Alizadeh, T., Ganjali, R.M., Zare, M., Norouzi, P. 2010. Development of a voltammetric sensor based on a molecularly imprinted polymer (MIP) for caffeine measurement. *Electrochimica Acta*, 55: 1568–1574.
- Altinc, G., Boz, I., Akturk, S.J. 2008. Synthesis and characterization of nanosized Cu/ZnO catalyst by polyolmethod. *Journal of Nanoscience and Nanotechnology*, 8(2): 874– 877.
- Alwarthan, A.A. 1993. Determination of ascorbic acid by flow injection with chemiluminescence detection. *Analyst*, 118: 639–642.
- An, G., Zhang, Y., Liu, Z., Miao, Z., Han, B., Bhushan, B., Theunissen, G. 2008. Preparation of porous chromium oxide nanotubes using carbon nanotubes as templates and their application as an ethanol sensor. *Nanotechnology*, 311: 67-80.
- Arvand, M., Sohrabnezhad, Sh., Mousavi, M.F., Shamsipur, M., Zanjanchi, M.A. 2003. Electrochemical study of methylene blue incorporated into mordenite type zeolite and its application for amperometric determination of ascorbic acid in real samples. *Analytica Chimica Acta*, 491: 193–201.
- Arya, P.S., Mahajan, M., Jain, P. 2000. Non-spectrophotometric methods for the determination of Vitamin C, *Analytica Chimica Acta*, 417: 1-14.
- Asnaashariisfahani, M., Karimi-maleh, H., Ahmar, H., Ensafi, AA., Fakhari, AR., Khalilzadeh, MA., Karimi, F. 2012. Novel 8, 9-dihydroxy-7-methyl-12H-benzothiazolo[2,3-

- b]quinazolin-12-one multiwalled carbon nanotubes paste electrode for simultaneous determination of ascorbic acid, acetaminophen and tryptophan. *Analytical Methods*, 4: 3275-3282.
- Astruc, D. 2004. *Inorganic Electrochemistry. Theory, Practice and Application*. Wiley Online Library.
- Baghayeri, M., Namadchian, M. 2013. Fabrication of a nanostructured luteolin biosensor for simultaneous determination of levodopa in the presence of acetaminophen and tyramine: Application to the analysis of some real samples. *Electrochimica Acta*, 108(1): 22-31.
- Baghizadeh, A., Karimi-Maleh, H., Khoshnama, Z., Hassankhani, A., Abbasghorbani, M. 2015. A voltammetric sensor for simultaneous determination of Vitamin C and Vitamin B<sub>6</sub> in food samples using ZrO<sub>2</sub> nanoparticle/Ionic liquids carbon paste electrode. *Food analytical methods*, 8: 549–557.
- Bard, A.J., Faulkner, L.R., Leddy, J., Zoski, C.G. 1980. *Electrochemical methods: fundamentals and applications*. Vol. 2., wiley New York.
- Basic overview of the working principle of a potentiostat/galvanostat (PGSTAT)– Electrochemical cell setup. Metrohm Autolab. BV, 2011: p. 1-3.
- Basics of Electrochemical Impedance Spectroscopy, in Application Note AC-1. Princeton Applied Research. p. 1 - 13.
- Beitollahi, H., Karimi-Maleh, H., Khabazzadeh, H. 2008. Nanomolar and Selective Determination of Epinephrine in the Presence of Norepinephrine Using Carbon Paste Electrode Modified with Carbon Nanotubes and Novel 2-(4-Oxo-3-phenyl-3,4-dihydroquinazoliny)-N'-phenyl-hydrazinecarbothioamide. *Analytical Chemistry*, 24: 9848-9851.
- Beitollahi, H., Nekooei, S. 2016. Application of a Modified CuO Nanoparticles Carbon Paste Electrode for Simultaneous Determination of Isoperrenaline, Acetaminophen and N-acetyl-L-cysteine. *Electroanalysis*, 28: 645-653.
- Bennici, A., Gervasini, and Ragaini, V. 2003. Preparation of highly dispersed CuO catalysts on oxide supports for de-NO(x) reactions. *Ultrasonic Son Chemistry*, 10(2): 61–64.
- Bijad, M., Karimi-Maleh, H., Khalilzadeh, M.A. 2013. Application of ZnO/CNTs nanocomposite ionic liquid paste electrode as a sensitive voltammetric sensor for determination of ascorbic acid in food samples. *Food Analytical Methods*, 6:1639–1647.

- Bilton, M., Steven, J., Andrew, M., Brown, P. 2012. Comparison of Hydrothermal and Sol-Gel Synthesis of Nano-Particulate Hydroxyapatite by Characterisation at the Bulk and Particle Level. *Journal of Inorganic Non-metallic Materials*, 2: 1-10.
- Bradshaw, P.M., Barril, C., Clark, C.A., Prenzler, P.D., Scollary, R.G. 2011. Ascorbic acid: A review of its chemistry and reactivity in relation to a wine environment. *Critical reviews in food science and nutrition*, 51:479-498.
- Brinker, C.J., Bunker, B.C., Tallant, D.R., Ward, K.J., Kirkpatrick, R.J. 1988. Structure of sol-gel derived inorganic polymers: silicates and borates, ACS symposium series. Chapter 26, 360: 314-332.
- Brinker, C.J., Scherer, S.W. 1990. Sol-Gel science: the physics and chemistry of sol-gel processing. Academic Press, New York.
- Carp, O., Huisman, C.L. and Reller, A. 2004. Photoinduced reactivity of titanium dioxide. *Progress in Solid State Chemistry*, 32: 33-177.
- Chen, C.W., Unnikrishnan, B., Chen, M.S. 2012. Electrochemical oxidation and amperometric determination of isoniazid at functionalized multiwalled carbon nanotube modified electrode. *International Journal of Electrochemical Science*, 7: 9138-9149.
- Chen, S.M., Chzo, W.Y. 2006. Simultaneous voltammetric detection of dopamine and ascorbic acid using didodecyldimethylammonium bromide (DDAB) film-modified electrodes. *Journal of Electroanalytical Chemistry*, 587: 226-234
- Chen, X., Mao, S.S. 2007. Titanium Dioxide Nanomaterials: Synthesis, Properties, Modifications and Applications. *Chemical Reviews*, 107: 2891-2959.
- Conley, J.M., Symes, S.J., Kindelberger, S.A., Richards, S.M. 2008. Rapid liquid chromatography tandem mass spectrometry method for the determination of a broad mixture of pharmaceuticals in surface water. *Journal of Chromatography A*, 1185: 206–215.
- Dalkiran, B., Kacar, C., Erden, E. P., Kilic, E. 2014. Amperometric xanthine biosensors based on chitosan CO<sub>3</sub>O<sub>4</sub> multiwall carbon nanotube modified glassy carbon electrode. *Sensors and Actuators B*, 200: 83-91.
- Danet, F.A., Badea, M., Aboul-Enein, Y.H. 2000. Flow injection system with chemiluminometric detection for enzymatic determination of ascorbic acid. *Luminescence* 15(5): 305-309.

- Dennison, D.B., Brawley, T.G., Hunter, G.L.K. 1981. Rapid high performance liquid chromatographic determination of ascorbic acid and combined ascorbic acid–dehydroascorbic acid in beverages. *Journal of Agricultural and Food Chemistry*, 29: 927–929.
- Deshmukh, S.G. and Bapat, G.M. 1955. Determination of ascorbic acid by potassium iodate. *Analytical Chemistry*, 145: 254.
- Elyasi, M., Khalilzadeh, MA., Karimi-Maleh, H. 2013. High sensitive voltammetric sensor based on Pt/CNTs nanocomposite modified ionic liquid carbon paste electrode for determination of Sudan I in food samples. *Food Chemistry*, 1419(4): 4311–4317.
- Ensafi, AA., Karimi-Maleh, H., Mallakpour, S., Rezaei, B. 2011. Highly sensitive voltammetric sensor based on catechol derivative multiwall carbon nanotubes for the catalytic determination of captopril in patient human urine samples. *Colloids and Surfaces B*, 87: 480–488.
- Ensafi, A.A., Karimi-Maleh, H., Mallakpour, S. 2012. Simultaneous determination of ascorbic acid, acetaminophen, and tryptophan by square wave voltammetry using N-(3,4-dihydroxyphenethyl)-3,5- dinitrobenzamide modified carbon nanotubes paste electrode. *Electroanalysis*, 24: 666–675.
- Fang, Y., Ni, Y., Zhang, G., Mao, C., Huang, X. and Shen, J. 2012. Biocompatibility of CS-PPy nanocomposites and their application to glucose biosensor. *Bio electrochemistry*, 88: 1-7.
- Fernandez-Sanchez, C., Costa-Garcia, A. 1997. Adsorption of immunoglobulin on carbon paste electrodes as a basis for the development of immune electrochemical devices. *Biosensor Bioelectronics*, 12: 403–413.
- Fekadu Tsegaye, 2016. Synthesis, Characterization and Sorption Property Study of Fe<sub>3</sub>O<sub>4</sub>/Al<sub>2</sub>O<sub>3</sub>/ZrO<sub>2</sub> Nanocomposites for the Removal of Cadmium, Lead and Uranium from Aqueous Solution. Thesis, Haramaya University.
- Ge, S., Shi, X., Sun, K., Li, C., Uher, C., Baker, J.R., Holl, M.B., Orr, B.G. 2009. Facile hydrothermal synthesis of iron oxide nanoparticles with tunable magnetic properties. *Journal of Physical Chemistry*, 113: 13593–13599.
- Girault, H.H., Analytical and physical electrochemistry. 2004: CRC Press.

- Gismera, M.J., Hueso, D., Procopio, J.R. and Sevilla, M.T. 2004. Ion-selective carbon paste electrode based on tetraethyl thiuram disulfide for copper (ii) and mercury (ii). *Analytica Chimica Acta*, 524: 347-353.
- Gholivand, B.M., Torkashvand, M., yavari, E. 2015. Electrooxidation behavior of warfarin in Fe<sub>3</sub>O<sub>4</sub> nanoparticles modified carbon paste electrode and its determination in real samples. *Materials Science and Engineering C*, 48: 235–242
- Goyal, R.N., Oyama, M., Gupta, V.K., Singh, S.P., Sharma, R.A. 2008. Sensors for 5- hydroxyl tryptamine and 5-hydroxyindole acetic acid based on nanomaterial modified electrodes. *Sensors and Actuators B*, 134: 816–821.
- Grabecsvogl, I., Kolar, M., Ogorevc, B. and Pihlar, B. 1998. Vermiculite clay mineral as an effective carbon paste electrode modifier for the preconcentration and voltammetric determination of Hg (II) and Ag (I) ions. *Journal of Analytical Chemistry*, 361: 358-362.
- Grudpan, K., Kamfoo, K., Jakmune, J. 1999. Flow injection spectrophotometric or conductometric determination of ascorbic acid in a vitamin C tablet using permanganate or ammonia. *Talanta*, 49: 1023–1026.
- Guclu, K., Sozgen, K., Tutem, E., Ozyurek, M., Apak, R. 2005. Spectrophotometric determination of ascorbic acid using copper (II) neocuproine reagent in beverages and pharmaceuticals. *Talanta*, 65: 1226–1232.
- Gupta, K.V., Jain, K.A., Khayat, A.M., Bhargava, K. S., Raison, R.J. 2008. Electroanalytical studies on Cobalt (II) selective potentiometric sensor based on bridge modified calixarene in poly (vinyl chloride). *Electrochimica Acta*, 53: 5409-5414.
- Han, R., Zou, L., Zhao, X., Xu, Y., Xu, F., Li, Y., Wang, Y. 2009. Characterization and properties of iron oxide-coated zeolite as adsorbent for removal of copper (II) from solution in fixed bed column. *Chemical Engineering Journal*, 149(1–3): 123–131.
- Harisha, V. K., Kumara Swamy, E. B., Jayadevappa, H., Vishwanath, C. C. 2015. Voltammetric Determination of Folic acid in presence of Dopamine and Ascorbic Acid at Poly (Alanine) Modified Carbon Paste Electrode. *Analytical and Bioanalytical Electrochemistry*, 7(4): 454-465.
- Hu, C.G., Wang, W.L., Feng, B., Wang, H. 2005. Simultaneous measurement of dopamine and ascorbic acid at CNT electrode. *International Journal of Modern Physics*, 19: 607-610.

- Hughes, E.D. 1983. Titrimetric determination of ascorbic acid with 2, 6-dichlorophenol indophenol in commercial liquid diets. *Journal of Pharmaceutical Sciences*, 72(2): 126-129.
- Hutton, A.E., Pauliukaite, R., Hocesvar, B.S., Ogorevc, B., Smyth, R.M. 2010. Amperometric microsensor for direct probing of ascorbic acid in human gastric juice. *Analytica Chimica Acta*, 678: 176-182.
- Jahani S., Beitollahi, H. 2016. Carbon paste electrode modified with  $\text{TiO}_2/\text{Fe}_3\text{O}_4/\text{MWCNT}$  nanocomposite and ionic liquids as a voltammetric sensor for sensitive ascorbic acid and tryptophan detection. *Analytical and Bioanalytical Electrochemistry*, 8(2): 158-168.
- Jamali, T., Karimi-Maleh, H., Khalilzadeh, M.A. 2014. A novel nanosensor based on Pt:Co nanoalloy ionic liquid carbon paste electrode for voltammetric determination of vitamin B<sub>9</sub> in food samples. *LWT-Food Science Technology*, 57: 679–685.
- Javanbakht, M., Fard, S.E., Abdouss, M., Mohammadi, A., Ganjali, M.R., Norouzi, P., Safaraliee, L. 2008. A biomimetic potentiometric sensor using molecularly imprinted polymer for the cetirizine assay in tablets and biological fluids. *Electroanalysis*, 20: 2023–2030.
- Javanbakht, M., Ganjali, M.R., Norouzi, P., Hashemi-Nasa, A., Badei, A.R. 2007. Carbon paste electrode modified with functionalized nanoporous silica gel as a new sensor for determination of silver ion. *Electroanalysis*, 19: 1307–1314.
- Jiang, H., Chen, P., Luo, S., Tu, X., Cao, Q., Shu, M. 2013. Synthesis of novel nanocomposite  $\text{Fe}_3\text{O}_4/\text{ZrO}_2/\text{chitosan}$  and its application for removal of nitrate and phosphate. *Applied Surface Science*, 284: 942-99.
- Jones, R.W. 1989. *Fundamental Principles of Sol-Gel Technology*. Institute of metals, London.
- Kadara, R.O, Jenkinson, N., Banks, C.E. 2009. Disposable bismuth oxide screen printed electrodes for the high throughput screening of heavy metals. *Electroanalysis*, 21: 2410-2414.
- Kalcher, K., Kauffmann, J.M., Wang, J., Svancara, I., Vytras, K., Neuhold, C., Yang, Z. 1995. Sensors based on carbon paste in electrochemical analysis: a review with particular emphasis on the period 1990–1993. *Electroanalysis*, 79: 5-22.

- Kamyabi, M.A. and Aghajanloo, F. 2008. Electrocatalytic oxidation and determination of nitrite on carbon paste electrode modified with oxovanadium (IV)-4-methyl salophen. *Journal of Electroanalytical Chemistry*, 614 (1–2): 157–165.
- Karimi-Maleh, H., Biparva, P., Hatami, M. 2013. A novel modified carbon paste electrode based on NiO/CNTs nanocomposite and (9,10-dihydro-9,10-ethanoanthracene-11,12-dicarboximido)-4-ethylbenzene-1,2-diol as a mediator for simultaneous determination of cysteamine, nicotin amide adenine dinucleotide and folic acid. *Biosensors and Bioelectronics*, 48: 270–275
- Karimi-Maleh, H., Biparva, P., Hatami, M. 2013. A novel modified carbon paste electrode based on NiO/CNTs nanocomposite and (9,10-dihydro-9,10-ethanoanthracene-11,12-dicarboximido)-4-ethylbenzene-1,2-diol as a mediator for simultaneous determination of cysteamine, nicotin amide adenine dinucleotide and folic acid. *Biosensors and Bioelectronics*, 48:270-275.
- Karimi-Maleh, H., Tahernejad-Javazmi, F., Daryanavard, M., Hadadzadeh, H., Ensafi, AA., Abbasghorbani, M. 2014. Electrocatalytic and simultaneous determination of ascorbic acid, nicotinamide adenine dinucleotide and folic acid at ruthenium (II) complex ZnO/CNTs nanocomposite modified carbon paste electrode. *Electroanalysis*, 26: 962-970.
- Kawakami, M.T., Tokunaga, Y., Yamamoto, H., Shibutani, Y. 2012. Ion selective electrodes based on l-tryptophan and l-tyrosine. *Talanta*, 94: 99-103.
- Keyvanfard, M., Shakeri, R., Karimi-Maleh, H., Alizad, K. 2013. Highly selective and sensitive voltammetric sensor based on modified multiwall carbon nanotube paste electrode for simultaneous determination of ascorbic acid, acetaminophen and tryptophan. *Materials Science and Engineering*, 33: 811–816.
- Khani, H., Rofouei, K.M., Arab, P., Gupta, K.V. Vafaei, Z. 2010. Multi-walled carbon nanotubes-ionic liquid-carbon paste electrode as a super selectivity sensor: application to potentiometric monitoring of mercury ion (II). *Journal of Hazardous Materials*, 183: 402-409.
- Kula, P., Navratilova, Z., Kulova, P., Kotoucek, M. 1999. Environmental analysis by electrochemical sensors and biosensors. *Analytica Chimica Acta*, 385: 91-101.

- Langley, E.C., B. Clukiz, B., Banks, E.C., Compton, G.R. 2007. Manganese dioxide graphite composite electrodes: application to the electroanalysis of hydrogen peroxide, ascorbic acid and nitrite. *Analytical Sciences*, 23(2): 165-170.
- Lavanya, M., Madhavi. G., Reddy, M.V.Y., Reddy, G.K., Jyothi, J.P. 2014. Electrochemical detection of dopamine in presence of uric acid using a zirconia modified carbon paste electrode. *International Journal of Applied, Physical and Bio-Chemistry Research* 4(3): 9-18.
- Li, F., Li, J., Feng, Y., Yang, L., Du, Z. 2011. Electrochemical behavior of graphene doped carbon paste electrode and its application for sensitive determination of ascorbic acid. *Sensors and Actuators B-Chemical*, 157: 110-114.
- Lin, C., Jie, W., Huangxian, J. 2015. Electrochemical sensing of heavy metal ions with inorganic, organic and bio-materials. *Biosensors and Bioelectronics*, 63: 276–286.
- Li, Y., Bai, Y., Han, G., Li, M. 2013. Porous reduced graphene oxide for fabricating an amperometric acetylcholinesterase biosensor. *Sensors and Actuators B*, 185: 706-712.
- Lu, H.C., Lu, J.L., Chu, C.L., Lai, C.Y. and Wu, G.M. 2008. Preparation of nano-powders of p-type transparent conductive copper aluminum oxide by co-precipitation method. In *Proceedings of the 2<sup>nd</sup> IEEE International Nanoelectronics Conference (INEC08)*, 485-488 March 2008. Shanghai, China.
- Lu, X., Wang, Z., Geng, Z., Kang, J., Gao, J. 2000. Electroanalysis with Carbon Paste Electrodes. *Talanta*, 52: 411-416.
- Lv, W.Z., Liu, B., Luo, Z.K., Ren, X.Z. and Zhang, P.X. 2008. XRD studies on the nanosized copper ferrite powders synthesized by sonochemical method. *Journal of Alloys and Compounds*, 465(1-2): 261-264.
- Lykkesfeldt, J. 2000. Determination of ascorbic acid and dehydro ascorbic acid in biological samples by high performance liquid chromatography using subtraction methods; reliable reduction with tris [2-carboxyethyl] phosphine hydrochloride. *Analytical Biochemistry*, 282: 89–93.
- Mabbott, G.A. 1983. An introduction to cyclic voltammetry. *Journal of Chemical Education*, 60(9): 697-702.

- Manoj, D., Satheesh, D., Santhanalakshmi, J. 2011. Reactive template method for the synthesis of Pd nanoparticles supported PoPd hollow spheres for electrochemical oxidation of ascorbic acid. *Transactions of the Indian Institute of Metals*, 64(1-2): 195.
- Maureen, R., Val-Vallyathan, G. 2006. Nanoparticles Health Effects. *Pros and Cons Environmental Health Perspectives*, 114(12): 1818- 1825.
- Monk, P.M. 2008. Fundamentals of electro-analytical chemistry. Vol. 29. John Wiley & Sons.
- Moradi, R., Sebt, S.A., Karimi-Maleh, H., Sadeghi, R., Karimi, F., Bahari, A., Arabi, H. 2013. Synthesis and application of FePt/CNTs nanocomposite as a sensor and novel amide ligand as a mediator for simultaneous determination of glutathione, nicotinamide adenine dinucleotide and tryptophan. *Physical Chemistry Chemical Physics*, 15(16): 5888-5897.
- Mousavi, M.F., Rahmani, A., Golabi, S.M., Shamsipur, M., Sharghi, H. 2001. Environmental applications of nanomaterials. *Talanta*, 55: 305-312.
- Najafi, M., Khalilzadeh, M.A., Karimi-Maleh, H. 2014. A new strategy for determination of bisphenol A in the presence of Sudan I using a ZnO/CNTs/ionic liquid paste electrode in food samples. *Food Chemistry*, 158: 125–131.
- Navratilova, Z. and Kula, P. 2000. Cation and anion exchange on clay modified electrodes. *Journal of Solid State Electrochemistry*, 4: 342–347.
- Nejad, G.F., Beitollahi, H., Shakeri, S. 2016. Magnetic Core shell Fe<sub>3</sub>O<sub>4</sub>/SiO<sub>2</sub>/Graphene Nanocomposite Modified Carbon Paste Electrode for Voltammetric Determination of Ascorbic Acid in the presence of L-Cysteine. *Analytical and Bioanalytical Electrochemistry*, 8(3): 318-328.
- Nobrega, A.J., Lopes, S.J. 1996. Flow injection spectrophotometric determination of ascorbic acid in pharmaceutical products with the Prussian Blue reaction. *Talanta*, 43(6): 971-976.
- O'Connell, J.P., Gormally, C., Pravda, M., Guilbault, G.G. 2001. Development of an amperometric l-ascorbic acid (Vitamin C) sensor based on electropolymerised aniline for pharmaceutical and food analysis. *Analytica Chimica Acta*, 431; 239-247.
- Oliveira, J.E., Watson, G.D. 2001. Chromatographic techniques for the determination of putative dietary anticancer compounds in biological fluids. *Journal of Chromatography B*, 764: 3-25.

- Padayatty, J.S., Katz, A., Wang, H.Y., Eck, P., Kwon, O., Lee, H.J., Chen, L.S., Corpe, C. Dutta, A., Dutta, K.S., Levine, M. 2003. Vitamin C as an antioxidant; evaluation of its role in disease prevention, *Journal of the American College of Nutrition*, 22(1): 18-35.
- Pillai, V., Kumar, P., Hou, M. J., Ayyub, P. Shah, D.O. 1995. Preparation of nanoparticles of silver halides, superconductors and magnetic materials using water-in-oil micro emulsions as nonreactors. *Advances in Colloid and Interface Science*, 55: 241–269.
- Pisoschi, M.A., Cheregi, C.M., Danet, F.A. 2009. Total antioxidant capacity of some commercial fruit juices: electrochemical and spectrophotometrical approaches. *Molecules*, 14(1): 480-493.
- Pisoschi, M.A., Pop, A., Negulescu, Gh.P., Pisoschi, A. 2011. Determination of ascorbic acid content of some fruit juices and wine by voltammetry performed at Pt and Carbon Paste Electrodes, *Molecules*, 16(2): 1349-1365.
- Polkowska, M.H., Danko, B., Dybczynski, R., Ammerlaan, A.K., Bode, P. 2000. Effect of acid digestion method on cobalt determination in plant materials. *Analytica Chimica Acta*, 408: 89-95.
- Prabhu, S.V., Baldwin, R.P., Kryger, L. 1989. Environmental analysis by electrochemical sensors and biosensors. *Electroanalysis*, 1: 13-21.
- Pradhan, S.D., Sathaye, S.D. and Patil, K.R. 2001. Low temperature synthesis of lead zirconate and titanate powder by hydroxide co-precipitation in non-aqueous medium. *Material letter*, 48: 351-355.
- Pumera, M., Ambrosi, A., Bonanni, A., Chng, E. and Poh, H. 2010. Graphene oxide for electrochemical sensing and biosensing. *Trends in Analytical Chemistry*, 29: 954-965.
- Ramesh, P., Sampath, S. 2004. Selective determination of uric acid in presence of ascorbic acid and dopamine at neutral pH using exfoliated graphite electrodes. *Electroanalysis*, 16: 866–869.
- Randviir, E.P., Banks, C.E. 2013. Electrochemical impedance spectroscopy: an overview of bioanalytical applications. *Analytical Methods*, 5(5): 1098-1115.
- Rizzolo, A., Brambilla, A., Valsecchi, S., Eccher-Zerbini, P. 2002. Evaluation of sampling and extraction procedures for the analysis of ascorbic acid from pear fruit tissue, *Food Chemistry*, 77: 257-262.

- Roodbari Shahmiri, M., Bahari, A., Karimi-Maleh, H., Hosseinzadeh, R., Mirnia, N . 2013. Ethynylferrocene–NiO/MWCNT nanocomposite modified carbon paste electrode as a novel voltammetric sensor for simultaneous determination of glutathione and acetaminophen. *Sensor and Actuators B*, 177: 70–77.
- Sabzi, R.E., Pournaghi-Azar, M.H. 2005. Electrocatalytic determination of ascorbic acid on a glassy carbon electrode chemically modified with cobalt pentacyanonitrosylferrate. *Analytical Sciences*, 21: 689–692.
- Sadeghi, R., Karimi-Maleh, H., Bahari, A., Taghavi, M. 2013. A novel biosensor based on ZnO nanoparticle/1,3-dipropylimidazolium bromide ionic liquid modified carbon paste electrode for square wave voltammetric determination of epinephrine. *Physics and Chemistry of Liquids*, 51: 704–714.
- Sanati, A.L., Karimi-Maleh, H., Badiei, A., Biparva, P., Ensafi, A.A. 2014. A voltammetric sensor based on NiO/CNTs ionic liquid carbon paste electrode for determination of morphine in the presence of diclofenac. *Material Science and Engineering C*, 35: 379-385.
- Sandulescu, R., Mirel, S., Oprean, R., 2000. The development of spectrophotometric and electroanalytical methods for ascorbic acid and acetaminophen and their applications in the analysis of effervescent dosage forms. *Journal of pharmaceutical and biomedical analysis*, 23: 77–87.
- Shahrokhian, S., Hamzehloei, A., Thaghani, A., Mousavi, S.R. 2004. Electrocatalytic oxidation of 2-Thiouracil and 2-Thiobarbituric acid at a carbon paste electrode Modified with cobalt phthalocyanine. *Electroanalysis*, 16: 915-921.
- Sies, H., Stahl, W., Sundquist, R.A. 1992. Antioxidant functions of vitamins. Vitamins E and C, beta-carotene and other carotenoids. *Annals of New York academy of sciences*, 669: 7-20.
- Silva, F.D.D., Lopes, C.B., Kubota, L.T., Lima, P.R., Goulart, M.O.F. 2012. Poly xanthurenic acid modified electrodes: An amperometric sensor for the simultaneous determination of ascorbic and uric acids. *Sensors Actuators*, 168: 289.
- Silva, G.C., Luz, I., Francesc, X., Corma, A. and Garcia, H. 2010. Water stable zirconium benzene dicarboxylate metal-organic frameworks as photocatalysts for hydrogen generation. *Journal of European*, 16: 11133-11138.

- Skoog, A.D., West, M.D., Holler, J.F. 1998. Fundamentals of Analytical Chemistry, Saunders College Publishing, 7<sup>th</sup> Edition, Philadelphia, p 845.
- Skrovankova, S., Mlcek, J., Sochor, J., Baron, M., Kynicky, J., Jurikova, T. 2015. Determination of Ascorbic Acid by Electrochemical Techniques and other Methods. *International Journal of Electrochemical Science*, 10: 2421–2431.
- Soldatkin, O.O., Peshkova, M.V., Saiapina, Y.O., Kucherenko, S.I., Dudchenko, Y.O., Melnyk, G. V., Vasylenko, D. O., Semenycheva, M.L., Soldatkin, P. A., Dzyadevych, V. S. 2013. Development of conductometric biosensor array for simultaneous determination of maltose, lactose, sucrose and glucose. *Talanta*, 115: 200-207.
- Svancara, I., Vytras, K., Kalcher, K., Walcarius, A., Wang, J. 2009. Carbon Paste Electrodes in Facts, Numbers, and Notes: A Review on the Occasion of the 50-Years Jubilee of Carbon Paste in Electrochemistry and Electroanalysis. *Electroanalysis*, 21: 7-28.
- Svancara, I., Vytras, K.I., Barek, J., Zima, J. 2001. Carbon paste electrodes in modern electroanalysis. *Critical Review of Analytical Chemistry*, 31: 311-345.
- Sun, W., Wang, Y., Lu, Y., Hu, A., Shi, F., Sun, Z. 2013. High sensitive simultaneously electrochemical detection of hydroquinone and catechol with a poly (crystal violet) functionalized graphene modified carbon ionic liquid electrode, *Sensors and Actuators B*, 188: 564-570.
- Tabata, M., Morita, H. 1997. Spectrophotometric determination of a nanomolar amount of ascorbic acid using its catalytic effect on copper (II) porphyrin formation. *Talanta*, 44: 151–157.
- Tesfaye Waryo, Qwasha, S., Baker, G.P., Emmanuel I. Iwuoha. 2016. Electrode Material Properties and Modelling of 1-Methyl-3-octylimidazolium imide Ionic Liquid/ Paraffin Carbon Pastes. *International Journal of Electrochemical Science*, 11: 4410-4426.
- Tuzen, M., Sari, H. and Soylak, M. 2004. Microwave and wet digestion procedures for atomic absorption spectrometric determination of trace metals contents of sediment samples. *Analytical Letters*, 37: 1949-1960.
- Ventra, M.D(ed)., Evoy, S. and Heflin, J.R. 2004. Introduction to Nanoscale Science and Technology. *Springer*, Page: 199-208.

- Vermeir, S., Hertog, M.T.A.L.M., Schenk, A., Beullens, K., Nicolai, M.B. Lammertyn, J. 2008. Evaluation and optimization of high-throughput enzymatic assays for fast l-ascorbic acid quantification in fruit and vegetables, *Analytica Chimica Acta*, 618: 94-101.
- Vasanth, V.S., Chen, S.M. 2006. Electrocatalysis and simultaneous detection of dopamine and ascorbic acid using poly (3,4-ethylenedioxy) thiophene film modified electrodes. *Journal of Electroanalytical Chemistry*, 592: 77-87.
- Vazquez, D., Tascón, M., Deban, L. 2012. Determination of Ascorbic Acid in Commercial Juices, on a Modified Carbon Paste Electrode, by Using a Taguchi Experimental Design. *Food Analytical Methods*, 5: 441–447.
- Wang, H., Xu, X., Zhang, J. and Li, C. 2010. A Cost-Effective Co-precipitation Method for Synthesizing Indium Tin Oxide Nanoparticles without Chlorine Contamination. *Journal of Material Science and Technology*, 26: 1037-1040.
- Wang, J. 2000. Applications of self-assembled monolayers in electroanalytical chemistry “Electroanalytical Chemistry,” 2<sup>nd</sup> Edition. Wiley, New York.
- Wang, J., Cai, X.H., Wang, J.Y., Jonsson, C., Palecek, E. 1995. Trace measurements of RNA by potentiometric stripping analysis at carbon paste electrodes. *Analytical Chemistry*, 67: 4065-4070.
- Wang, Y., Wei, W.Z., Liu, X.Y., Zeng, X.D. 2008. Fabrication of a copper nanoparticle/chitosan/carbon nanotube-modified glassy carbon electrode for electrochemical sensing of hydrogen peroxide and glucose. *Microchim Acta*, 160: 253–260.
- Wei, H., Sun, H., Wang, S. 2010. Low temperature H<sub>2</sub>S sensor based on copper oxide/tin dioxide thick film. *Journal of Natural Gas Chemistry*, 19(4): 393–396.
- Wen, L.X., Han, X.Z., Rieker, A., Liu, L.Z. 1997. Significant micellar effect on the oxidative electrochemistry of ascorbic acid. *Journal of chemical Research*, 3: 108-109.
- Wilson, G.S., Gifford, R. 2005. Biosensors for real-time in vivo measurements. *Biosensors and Bioelectronics*, 20: 2388-2403.
- Wu, R., Qu, J., He, H. and Yu, Y. 2003. Preparation and characterization of Cu catalysts supported on organized mesoporous alumina. *Journal of Beijing University of Chemical Technology (Natural Science Edition)*, 48: 2311–2316.

- Xu, J.Z., Zhu, J.J., Wang, H. and Chen, H.Y. 2003. Nano-sized copperoxide modified carbon paste electrodes as an amperometric sensor for amikacin. *Analytical Letters*, 36(13): 2723–2733.
- Yang, J., He, M., Hu, X. 2011. Copper oxide nanoparticle sensors for hydrogen cyanide detection: unprecedented selectivity and sensitivity. *Sensors and Actuators B*, 155(2): 692–698.
- Yang, J., Mei, S., Ferreira, J. M. F. 2001. Hydrothermal and synthesis of TiO<sub>2</sub> nanopowders from tetraalkylammonium hydroxide peptidedsols. *Material Science and Engineering C: Journal*, 15: 183-185.
- Yang, Y., Zhou, J., Zhang, H., Gai, P., Zhang, X., Chen, J. 2013. Electrochemical evaluation of total antioxidant capacities in fruit juice based on the guanine/graphene nanoribbon/glassy carbon electrode. *Talanta*, 106: 206-211.
- Yola, M.L., Gupta, V.K., Eren, T., Sen, AE., Atar, N. 2014. A novel electroanalytical nanosensor based on graphene oxide/silver nanoparticles for simultaneous determination of quercetin and morin. *Electrochimica Acta*, 120: 204–211.
- Yola, M.L., Atar, N. 2014. A novel voltammetric sensor based on gold nanoparticles involved in p-aminothiophenol functionalized multiwalled carbon nanotubes; Application to the simultaneous determination of quercetin and rutin. *Electrochimica Acta*, 119: 24–31.
- Yola L.M, Atar, N., Ustundag, Z., Solak, A.O. 2013. A novel voltammetric sensor based on p-amino thiophenol functionalized grapheme oxide/gold nanoparticles for determining quercetin in the presence of ascorbic acid. *Journal of Electroanalytical Chemistry*, 698: 9–16.
- Yuan, L., Jiang, L., Liu, J., Xia, Z., Wang, S., Sun, G. 2014. Facile synthesis of silver nanoparticles supported on three dimensional graphene oxide/carbon black composite and its application for oxygen reduction reaction. *Electrochimica Acta*, 135: 168-174.
- Zanello, P. 2007. Inorganic Electrochemistry. Theory, Practice and Application. Royal Society of Chemistry.
- Zen, J.M, Tsai, D.M, Kumar, A.S, Dharuman, V. 2000. Amperometric determination of ascorbic acid at a ferricyanide doped Tosflex modified electrode. *Electrochemical Communications*, 2: 782.

- Zeng, W., Martinuzzi, F., MacGregor, A. 2005. Development and application of a novel UV method for the analysis of ascorbic acid. *Journal of Pharmaceutical and Bioanalytical Chemistry*, 36: 1107–1111.
- Zhang, K., Song, G., Li, Y., Wu, X., Li, K., Ye, B. 2014. Voltammetric studies of kaempferol on polyvinyl pyrrolidone cladding quantum dots CdS doped carbon paste electrode and analytical application. *Sensors and Actuators B*, 191: 673- 680.
- Zhang, S., Wang, N., Niu, Y., Sun, C. 2005. Immobilization of glucose oxidase on gold nanoparticles modified Au electrode for the construction of biosensor. *Sensors and Actuators. B*. 109: 367-374.
- Zhang, Z., Qin, W. 1996. Chemiluminescence flow sensor for the determination of ascorbic acid with immobilized reagents. *Talanta*, 43: 119–124.
- Zhang, L., Sun, Y., Lin, X., 2001. Separation of anodic peaks of ascorbic acid and dopamine at an  $\alpha$ -alanine covalently modified glassy carbon electrode. *Analyst*, 126: 1760–1763.
- Zhang, Z.J., Li, X., Wang, C.G., Zhang, C.C., Liu, P., Fang, T.T., Xiong, Y., Xu, W.J. 2012. A novel binuclear Schiff-base copper (II) complex modified electrode for ascorbic acid catalytic oxidation and determination. *Dalton Trans*, 41: 1252-1258.
- Zhao, Y., Gao, Y., Zhan, D., Hui, H., Zhao, Q., Kou, Y., Shao, Y., Li, M., Zhuang, Q., Zhu, Z. 2005. Selective detection of dopamine in the presence of ascorbic acid and uric acid by a carbon nanotubes ionic liquid gel modified electrode. *Talanta*, 66: 51-57.
- Zidan, M., Tan, T.W., Zainal, Z., Abdullah, H.A., Goh, K.J. 2011. Electrochemical oxidation of ascorbic acid mediated by Bi<sub>2</sub>O<sub>3</sub> microparticles modified glassy carbon electrode. *International Journal of Electrochemical Science*, 6: 289-300.
- Zou, W., Han, R., Chen, Z., Shi, J., Hongmin, L. 2006. Characterization and properties of manganese oxide coated zeolite as adsorbent for removal of copper (II) and lead (II) ions from solution. *Journal of Chemical and Engineering Data*, 51(2): 534–541.

## **7. APPENDIXES**

Table 1. Reproducibility Fe<sub>3</sub>O<sub>4</sub>/ZrO<sub>2</sub>/CPE

Trial	Ipa	% Detection	% RSD
1	17.5	100	
2	17.52	100.1	
3	17.47	99.8	2.4
4	17.46	99.77	
5	17.49	99.9	

Table 2. Stability Fe<sub>3</sub>O<sub>4</sub>/ZrO<sub>2</sub>/CPE

Day	Ipa
6	17.5
12	17.2
18	17.09
24	17.01
30	16.96